

Cite as: M. Yuan *et al.*, *Science* 10.1126/science.abh1139 (2021).

# Structural and functional ramifications of antigenic drift in recent SARS-CoV-2 variants

Meng Yuan<sup>1†</sup>, Deli Huang<sup>2†</sup>, Chang-Chun D. Lee<sup>1†</sup>, Nicholas C. Wu<sup>3,4†</sup>, Abigail M. Jackson<sup>1</sup>, Xueyong Zhu<sup>1</sup>, Hejun Liu<sup>1</sup>, Linghang Peng<sup>2</sup>, Marit J. van Gils<sup>5</sup>, Rogier W. Sanders<sup>5,6</sup>, Dennis R. Burton<sup>2,7</sup>, S. Momsen Reincke<sup>8,9</sup>, Harald Prüss<sup>8,9</sup>, Jakob Kreye<sup>8,9</sup>, David Nemazee<sup>2</sup>, Andrew B. Ward<sup>1</sup>, Ian A. Wilson<sup>1,10\*</sup>

<sup>1</sup>Department of Integrative Structural and Computational Biology, The Scripps Research Institute, La Jolla, CA 92037, USA. <sup>2</sup>Department of Immunology and Microbiology, The Scripps Research Institute, La Jolla, CA 92037, USA. <sup>3</sup>Department of Biochemistry, University of Illinois at Urbana-Champaign, Urbana, IL 61801, USA. <sup>4</sup>Carl R. Woese Institute for Genomic Biology, University of Illinois at Urbana-Champaign, Urbana, IL 61801, USA. <sup>5</sup>Department of Medical Microbiology and Infection Prevention, Amsterdam University Medical Centers, Location AMC, University of Amsterdam, Amsterdam, Netherlands. <sup>6</sup>Department of Microbiology and Immunology, Weill Medical College of Cornell University, New York, NY 10021, USA. <sup>7</sup>Ragon Institute of MGH, Harvard, and MIT, Cambridge, MA 02139, USA. <sup>8</sup>German Center for Neurodegenerative Diseases (DZNE) Berlin, Berlin, Germany. <sup>9</sup>Department of Neurology and Experimental Neurology, Charité-Universitätsmedizin Berlin, corporate member of Freie Universität Berlin, Humboldt-Universität Berlin, and Berlin Institute of Health, Berlin, Germany. <sup>10</sup>Skaggs Institute for Chemical Biology, The Scripps Research Institute, La Jolla, CA 92037, USA.

†These authors contributed equally to this work.

\*Corresponding author. Email: wilson@scripps.edu

**Neutralizing antibodies (nAbs) elicited against the receptor-binding site (RBS) of the spike protein of wild-type SARS-CoV-2 are generally less effective against recent variants of concern. RBS residues E484, K417 and N501 are mutated in variants first described in South Africa (B.1.351) and Brazil (P.1). We analyzed their effects on ACE2 binding and K417N and E484K mutations on nAbs isolated from COVID-19 patients. Binding and neutralization of the two most frequently elicited antibody families (IGHV3-53/3-66 and IGHV1-2), which can both bind the RBS in alternate binding modes, are abrogated by K417N, E484K, or both. These effects can be structurally explained by their extensive interactions with RBS nAbs. However, nAbs to the more conserved, cross-neutralizing CR3022 and S309 sites were largely unaffected. The results have implications for next-generation vaccines and antibody therapies.**

The COVID-19 pandemic has already lasted for over a year, but new infections are still escalating throughout the world. While several different COVID-19 vaccines have been deployed globally, a major concern is the emergence of antigenically distinct SARS-CoV-2 variants of concern (VOCs). In particular, the B.1.1.7 lineage that arose in the UK (*1*) and quickly became dominant, B.1.351 (also known as 501Y.V2) lineage in South Africa (*2*), B.1.1.28 lineage (and its descendant B.1.1.28.1, aka P.1/501Y.V3) in Brazil (*3*), and B.1.232/B.1.427/B.1.429 (aka CAL.20C and CAL.20A) in the United States (*4*) have raised serious questions about the nature, extent and consequences of antigenic drift in SARS-CoV-2. In the receptor-binding site (RBS) of the spike (S) protein receptor-binding domain (RBD), the B.1.1.7 lineage has acquired an N501Y mutation, B.1.351 and P.1 lineages share this mutation along with K417N/T and E484K, whereas the California variants have an L452R mutation that is also present in the Indian variant B.1.617 with E484Q (*5*).

E484K has also been detected in a few B.1.1.7 genomes (*1*) (Fig. 1A). We therefore investigated the structural and functional consequences of such mutations on neutralizing antibodies (nAbs) isolated from COVID-19 convalescent patients, and their effect on angiotensin-converting enzyme 2 (ACE2) receptor binding.

N501Y was previously reported to enhance binding to human receptor ACE2 (*6, 7*). Here, we quantified binding of K417N, E484K, N501Y, and double and triple combinations in the RBD to ACE2 by biolayer interferometry (Fig. 1A and fig. S1). N501Y indeed increased RBD binding to ACE2 compared to wild-type RBD ( $K_D$  3.3 nM vs 7.0 nM), whereas K417N substantially reduced ACE2 binding (41.6 nM). E484K slightly reduced binding (11.3 nM). Importantly, N501Y could rescue binding of K417N (9.0 nM), and the triple mutant K417N/E484K/N501Y (as in B.1.351) had similar binding (6.5 nM) to wild type (Fig. 1A and fig. S1). Consistently, K417N/T mutations are associated with N501Y in nat-

urally circulating SARS-CoV-2. Among 585,054 SARS-CoV-2 genome sequences in the GISAID database (March 5, 2021) (8), about 95% of K417N/T mutations occur with N501Y, despite N501Y being present in only 21% of all analyzed sequences. In contrast, only 36% of E484K mutations occur with N501Y.

We and others have shown that most SARS-CoV-2 nAbs that target the RBD and their epitopes can be classified into different sites and subsites (9–12). Certain IGHV genes are highly enriched in the antibody response to SARS-CoV-2 infection, with IGHV3-53 (11, 13–16) and IGHV3-66, which differ by only one conservative substitution (V12I), and IGHV1-2 (11, 17, 18) being the most enriched IGHV genes used among 1,593 RBD-targeting antibodies from 32 studies (11, 14–44) (Fig. 1B). We investigated the effects of the prevalent SARS-CoV-2 mutations on neutralization by these multi-donor class antibodies, and the consequences for current vaccines and therapeutics.

K417N and E484K in VOCs B.1.351 and P.1 have been reported to decrease the neutralizing activity of sera as well as neutralizing monoclonal antibodies isolated from COVID-19 convalescent plasma and vaccinated individuals (45–62). B.1.351 is ~8–14 fold and P.1 is ~2.6–5 fold more resistant to neutralization by convalescent plasma and mRNA vaccinee sera (63–68). Some variants are able to escape neutralization by some nAbs (e.g., LY-CoV555, 910-30, COVOX-384, S2H58, C671, etc.) while others retain activity (e.g., 1-57, 2-7, mAb-222, S309, S2E12, COV2-2196, C669, etc.) (50, 57, 63, 66, 69, 70). Here, we selected a representative panel of 17 human nAbs isolated from COVID-19 patients or humanized mice to study the escape mechanism. These nAbs cover all known neutralizing sites on the RBD and include those encoded by V genes that are the most frequently used and also significantly enriched (Fig. 1B). We tested the activity of a panel of nAbs against wild-type (Wuhan strain) SARS-CoV-2 pseudovirus and single mutants K417N and E484K (Fig. 1C). Binding and neutralization of four and five antibodies out of the 17 tested were abolished by K417N and E484K, respectively. Strikingly, binding and neutralization by all six highly potent IGHV3-53 antibodies (71) that we tested were abrogated by either K417N (RBS-A/class 1) or E484K (RBS-B/class 2) (Fig. 1, C and D, and fig. S2). In addition, binding and neutralization of IGHV1-2 antibodies was severely reduced for the E484K mutation (Fig. 1, C and D, and fig. S2).

We next examined 54 SARS-CoV-2 RBD-targeting human antibodies with available structures. The antibody epitopes on the RBD can be classified into six sites: four RBS subsites RBS-A, B, C, and D; CR3022 site; and S309 site (fig. S3) (72), that are related to the four classes assigned in (10) (Fig. 1C). Twenty one of 23 IGHV3-53/3-66 antibodies target RBS-A (Fig. 2A). All IGHV1-2 antibodies with structures to date bind to the RBS-B epitope. A large fraction of

antibodies in these two main families make contact with K417, E484 or N501 in their epitopes (Fig. 2A) (73). Almost all RBS-A antibodies interact extensively with K417 and N501, whereas most RBS-B and RBS-C antibodies contact E484, and most RBS-C antibodies interact with L452. We also examined the buried surface area (BSA) of K417, E484, and N501 upon interaction with these RBD-targeting antibodies (fig. S3C). The extensive BSA confirmed why mutations at 417 and 484 affect binding and neutralization. Antibodies targeting RBS-D, or the cross-neutralizing S309 and CR3022 sites, are minimally or not involved in interactions with these four RBD mutations (Fig. 2A and fig. S3C).

IGHV3-53/3-66 RBD antibodies can adopt two different binding modes (9, 10), which we refer here to as binding modes 1 and 2 (74), with distinct epitopes and approach angles (Fig. 2B and fig. S4). All IGHV3-53/3-66 RBD antibodies to date with binding mode 1 have a short CDR H3 of <15 amino acids and bind RBS-A (13, 16, 32), while those with binding mode 2 have a longer CDR H3 ( $\geq$ 15 amino acids) and target RBS-B (9, 10, 75). These dual binding modes enhance recognition of this antibody family for the SARS-CoV-2 RBD, although most IGHV3-53/3-66 RBD antibodies adopt binding mode 1 (Fig. 2 and fig. S4). K417 is a key epitope residue for antibodies with IGHV3-53/3-66 binding mode 1 (Fig. 2B and fig. S4). IGHV3-53 germline residues V<sub>H</sub> Y33 and Y52 make hydrophobic interactions with the aliphatic moiety of K417, and its ε-amino group interacts with CDR H3 through a salt bridge (D97 or E97), hydrogen bond (H-bond), or cation-π interaction (F99) (Fig. 2B). K417N/T would diminish such interactions and, therefore, affect antibody binding and neutralization, providing a structural explanation for K417N escape in IGHV3-53/3-66 antibodies with binding mode 1 (Fig. 1, C and D, Fig. 2B, and fig. S2). In contrast, IGHV3-53 antibodies with binding mode 2 do not interact with RBD-K417 (fig. S4), but with E484 through H-bonds with CDRH2 (Fig. 2C). Consistently, binding and neutralization of IGHV3-53 antibodies with binding mode 2 (fig. S4) are abolished by E484K, but not K417N (Fig. 1, C and D, and fig. S2). Interestingly, unlike most IGHV3-53 antibodies that are sensitive to K417N/T or E484K, a recently discovered IGHV3-53-encoded mAb-222, which binds RBS retains activity against P.1 and B.1.351. The mAb-222 light chain could largely restore the neutralization potency of other IGHV3-53 antibodies, suggesting that light-chain interactions can compensate for loss of binding of K417N/T by the heavy chain (63). However, this antibody may represent only a small portion of IGHV3-53/3-66 antibodies that can neutralize VOCs.

Among the IGHV genes used in RBD antibodies, IGHV1-2 is also highly enriched over the baseline frequency in the antibody repertoire of healthy individuals (76), and is second only to IGHV3-53/3-66 (Fig. 1B). We compared three

structures of IGHV1-2 antibodies, namely 2-4 (27), S2M11 (30), and C121 (10), that target RBS-B. Despite being encoded by different IGK(L)V genes, 2-4 (IGLV2-8), S2M11 (IGKV3-20), and C121 (IGLV2-23) share a nearly identical binding mode and epitope (Fig. 3A). Structural analysis reveals that the  $V_H^{26}$ GYTFTG(Y) $Y^{33}$ ,  $^{50}W(I)N/S(P)XSXGTX^{58}$ ,  $^{73}TS(I)S/T^{76}$  motifs are important for RBD binding (fig. S5, A to D). Although only a small part of the epitope interacts with the light chains of 2-4, S2M11, and C121,  $V_L$  32 and 91 (n.b. also residue 30 in some antibodies) play an important role in forming a hydrophobic pocket together with  $V_H$  residues for binding RBD-F486, which is another key binding residue in such classes of antibodies (9) (fig. S5, E to I). Three other IGHV1-2 antibodies, 2-43, 2-15, and H4, also bind in a similar mode (77), further highlighting structural convergence of IGHV1-2 antibodies in targeting the same RBD epitope. Importantly, all IGHV1-2 antibodies to date form extensive interactions with E484 (Fig. 3A and fig. S3C). In particular, germline-encoded  $V_H$  Y33, N52 (somatically mutated to S52 in C121) and S54 are involved in polar interactions with the RBD-E484 side chain that would be altered by substitution with Lys (Fig. 3A) and thereby diminish binding and neutralization of IGHV1-2 antibodies against E484K (Fig. 1, C and D, and fig. S2).

We previously isolated another potent IGHV1-2 antibody, CV05-163, targeting the SARS-CoV-2 RBD (fig. S6) from a COVID-19 patient (17). CV05-163 likely represents a shared antibody response for IGHV1-2 RBD antibodies across patients (fig. S7). Negative-stain electron microscopy (nsEM) of CV05-163 in complex with the SARS-CoV-2 S trimer illustrates that it can bind in various stoichiometries, including molar ratios of 1:1, 2:1, and 3:1 (Fab to S protein trimer), and can accommodate RBDs in both up- and down-conformations (fig. S8). We also determined a crystal structure of Fab CV05-163 with SARS-CoV-2 RBD and Fab CR3022 to 2.25 Å resolution (Fig. 3B, figs. S9 to S11, and tables S1 and S2) and found that it does indeed bind RBS-B (Fig. 3) and makes extensive interactions with E484 through H-bonds ( $V_H$  W50 and  $V_H$  N58) and a salt bridge ( $V_L$  R91) (Fig. 3B) that explains why CV05-163 binding and neutralization were diminished with E484K (Fig. 1, C and D, and fig. S2). However, CV05-163 is rotated 90° (Fig. 3B) compared to other IGHV1-2 antibodies 2-4, S2M11, and C121 (Fig. 3A). Thus, IGHV1-2 antibodies, akin to IGHV3-53/66 (75), can engage the RBD in two different binding modes, both of which are susceptible to escape by E484K, but not by K417N (Fig. 1, C and D).

A further group of antibodies target the back side of the RBS ridge (RBS-C) (9). To date, five nAbs isolated from COVID-19 patients are known to bind RBS-C: CV07-270 (17), BD-368-2 (38), P2B-2F6 (18), C104 (10), and P17 (78). These RBS-C nAbs also interact with E484 (Fig. 4A), mainly

through an arginine in CDRH3, suggesting that E484K may adversely impact RBS-C antibodies. Indeed, binding and neutralization by CV07-270 was abrogated by E484K (Fig. 1C and fig. S2). Intriguingly, these five RBS-C antibodies are encoded by five different IGHV genes (79), but target a similar epitope with similar angles of approach. In addition, neutralization by REGN10933, a potent antibody used for therapeutic treatment, was reduced to a less extent by K417N and E484K (Fig. 1C) (28). REGN10933 binds at a slightly different angle from RBS-A antibodies and other RBS-B antibodies. K417 then interacts with CDRs H1 and H3 of REGN10933, whereas E484 contacts CDRH2 (fig. S12). Overall, our results demonstrate that RBS mutations K417N and E484K can either abolish or extensively reduce the binding and neutralization of several major classes of SARS-CoV-2 RBD antibodies.

Two other non-RBS sites that are distant from K417 and E484 have been repeatedly shown to be neutralizing sites on the SARS-CoV-2 RBD, namely the CR3022 cryptic site and S309 proteoglycan site (9) (Fig. 1C and Fig. 4B). Antibodies from COVID-19 patients can neutralize SARS-CoV-2 by targeting the CR3022 site, including COVA1-16 (80), S304, S2A4 (31), and DH1047 (41). Recently, we isolated antibody CV38-142 that targets the S309 site (81). Antibodies targeting these two epitopes are often cross-reactive with other sarbecoviruses, as these sites are more evolutionarily conserved compared to the RBS. To test the effect of the K417N and E484K mutations on nAbs that target the S309 and CR3022 sites, we assessed binding and neutralization by CV38-142 and COVA1-16 to SARS-CoV-2. Both mutations have minimal effect on these antibodies (Fig. 1C and Fig. 4C).

The most potent neutralizing antibodies to SARS-CoV-2 generally tend to target the RBS (table S3), as they directly compete with receptor binding. Such RBS antibodies often interact with K417, E484, or N501, which are located in the RBS, and are therefore sensitive to RBS mutations in the VOCs. On the other hand, antibodies targeting the CR3022 and S309 sites are often less potent, but are less affected by the VOCs, as their epitopes do not contain mutated residues. In fact, recent studies have shown that sera from convalescent or vaccinated individuals can retain neutralization activity, albeit reduced, against the mutated variants (48, 50, 82), which is possibly due to antibodies targeting other epitopes including the CR3022 and S309 sites. Thus, the CR3022 and S309 sites are promising targets to avoid interference by SARS-CoV-2 mutations observed to date.

As SARS-CoV-2 continues to circulate in humans and increasing numbers of COVID-19 vaccines are administered, herd immunity to SARS-CoV-2 should be approached locally and globally. However, as with other RNA viruses, such as influenza and HIV (83), further antigenic drift is anticipated

in SARS-CoV-2. Intra-host antigenic drift has also been observed in an immunosuppressed COVID-19 patient who had low titers of neutralizing antibodies that allowed emergence of N501Y and E484K mutations (84). While antibody responses elicited by the wild-type lineage that initiated the COVID-19 pandemic have been well characterized in natural infection (11, 14–18, 20, 23, 26, 27, 29) and vaccination (50, 85–87), data on the immune response to VOCs are now only starting to emerge (88) and will inform on the similarity and differences in the antibodies elicited. Since SARS-CoV-2 is likely to become endemic (89), the findings here and in other recent studies can be used to fast-track development of more broadly effective vaccines and therapeutics.

## REFERENCES AND NOTES

- M. Chand *et al.*, Investigation of Novel SARS-CoV-2 Variant: Variant of Concern 202012/01. Technical Briefing 5. Public Health England (2020); [https://assets.publishing.service.gov.uk/government/uploads/system/uploads/attachment\\_data/file/959426/Variant\\_of\\_Concern\\_VOC\\_202012\\_01\\_Technical\\_Briefing\\_5.pdf](https://assets.publishing.service.gov.uk/government/uploads/system/uploads/attachment_data/file/959426/Variant_of_Concern_VOC_202012_01_Technical_Briefing_5.pdf).
- H. Tegally *et al.*, Emergence and rapid spread of a new severe acute respiratory syndrome-related coronavirus 2 (SARS-CoV-2) lineage with multiple spike mutations in South Africa. medRxiv 20248640 [preprint]. 22 December 2020.
- N. R. Faria *et al.*, “Genomic characterisation of an emergent SARS-CoV-2 lineage in Manaus: preliminary findings” (2021); <https://virological.org/t/genomic-characterisation-of-an-emergent-sars-cov-2-lineage-in-manaus-preliminary-findings/586>.
- V. Tchesnokova, H. Kulakesara, L. Larson, V. Bowers, E. Rechkina, D. Kisiela, Y. Sledneva, D. Choudhury, I. Maslova, K. Deng, K. Kutumbaka, H. Geng, C. Fowler, D. Greene, J. Ralston, M. Samadpour, E. Sokurenko, Acquisition of the L452R mutation in the ACE2-binding interface of Spike protein triggers recent massive expansion of SARS-CoV-2 variants. bioRxiv 432189 [preprint]. 22 February 2021.
- P. D. Yadav, G. N. Sapkal, P. Abraham, R. Ella, G. Deshpande, D. Y. Patil, D. A. Nyayanit, N. Gupta, R. R. Sahay, A. M. Shete, S. Panda, B. Bhargava, V. K. Mohan, Neutralization of variant under investigation B.1.617 with sera of BBV152 vaccinees. *Clin. Infect. Dis.* ciab411 (2021). doi:10.1093/cid/ciab411
- X. Zhu, D. Mannar, S. S. Srivastava, A. M. Berezuk, J.-P. Demers, J. W. Saville, K. Leopold, W. Li, D. S. Dimitrov, K. S. Tuttle, S. Zhou, S. Chittori, S. Subramanian, Cryo-electron microscopy structures of the N501Y SARS-CoV-2 spike protein in complex with ACE2 and 2 potent neutralizing antibodies. *PLOS Biol.* 19, e3001237 (2021). doi:10.1371/journal.pbio.3001237 Medline
- T. N. Starr, A. J. Greaney, S. K. Hilton, D. Ellis, K. H. D. Crawford, A. S. Dingens, M. J. Navarro, J. E. Bowen, M. A. Tortorici, A. C. Walls, N. P. King, D. Veesler, J. D. Bloom, Deep mutational scanning of SARS-CoV-2 receptor binding domain reveals constraints on folding and ACE2 binding. *Cell* 182, 1295–1310.e20 (2020). doi:10.1016/j.cell.2020.08.012 Medline
- Y. Shu, J. McCauley, GISAID: Global initiative on sharing all influenza data - from vision to reality. *Euro Surveill.* 22, 30494 (2017). doi:10.2807/1560-7917.ES.2017.22.13.30494 Medline
- M. Yuan, H. Liu, N. C. Wu, I. A. Wilson, Recognition of the SARS-CoV-2 receptor binding domain by neutralizing antibodies. *Biochem. Biophys. Res. Commun.* 538, 192–203 (2021). doi:10.1016/j.bbrc.2020.10.012 Medline
- C. O. Barnes, C. A. Jette, M. E. Abernathy, K. A. Dam, S. R. Esswein, H. B. Gristick, A. G. Malyutin, N. G. Sharaf, K. E. Huey-Tubman, Y. E. Lee, D. F. Robbiani, M. C. Nussenzweig, A. P. West Jr., P. J. Bjorkman, SARS-CoV-2 neutralizing antibody structures inform therapeutic strategies. *Nature* 588, 682–687 (2020). doi:10.1038/s41586-020-2852-1 Medline
- T. F. Rogers, F. Zhao, D. Huang, N. Beutler, A. Burns, W. T. He, O. Limbo, C. Smith, G. Song, J. Woehl, L. Yang, R. K. Abbott, S. Callaghan, E. Garcia, J. Hurtado, M. Parren, L. Peng, S. Ramirez, J. Ricketts, M. J. Ricciardi, S. A. Rawlings, N. C. Wu, M. Yuan, D. M. Smith, D. Nemazee, J. R. Teijaro, J. E. Voss, I. A. Wilson, R. Andraibi, B. Briney, E. Landais, D. Sok, J. G. Jardine, D. R. Burton, Isolation of potent SARS-CoV-2 neutralizing antibodies and protection from disease in a small animal model. *Science* 369, 956–963 (2020). doi:10.1126/science.abc7520 Medline
- W. Dejnirattisai, D. Zhou, H. M. Ginn, H. M. E. Duyvesteyn, P. Supasa, J. B. Case, Y. Zhao, T. S. Walter, A. J. Mentzer, C. Liu, B. Wang, G. C. Paesen, J. Slon-Campos, C. López-Camacho, N. M. Kafai, A. L. Bailey, R. E. Chen, B. Ying, C. Thompson, J. Bolton, A. Fyfe, S. Gupta, T. K. Tan, J. Gilbert-Jaramillo, W. James, M. Knight, M. W. Carroll, D. Skelly, C. Dold, Y. Peng, R. Levin, T. Dong, A. J. Pollard, J. C. Knight, P. Klenerman, N. Temperton, D. R. Hall, M. A. Williams, N. G. Paterson, F. K. R. Bertram, C. A. Siebert, D. K. Clare, A. Howe, J. Radecke, Y. Song, A. R. Townsend, K. A. Huang, E. E. Fry, J. Mongkolsapaya, M. S. Diamond, J. Ren, D. I. Stuart, G. R. Screaton, The antigenic anatomy of SARS-CoV-2 receptor binding domain. *Cell* 184, 2183–2200.e22 (2021). doi:10.1016/j.cell.2021.02.032 Medline
- M. Yuan, H. Liu, N. C. Wu, C. D. Lee, X. Zhu, F. Zhao, D. Huang, W. Yu, Y. Hua, H. Tien, T. F. Rogers, E. Landais, D. Sok, J. G. Jardine, D. R. Burton, I. A. Wilson, Structural basis of a shared antibody response to SARS-CoV-2. *Science* 369, 1119–1123 (2020). doi:10.1126/science.abd2321 Medline
- Y. Cao, B. Su, X. Guo, W. Sun, Y. Deng, L. Bao, Q. Zhu, X. Zhang, Y. Zheng, C. Geng, X. Chai, R. He, X. Li, Q. Lv, H. Zhu, W. Deng, Y. Xu, Y. Wang, L. Qiao, Y. Tan, L. Song, G. Wang, X. Du, N. Gao, J. Liu, J. Xiao, X. D. Su, Z. Du, Y. Feng, C. Qin, C. Qin, R. Jin, X. S. Xie, Potent neutralizing antibodies against SARS-CoV-2 identified by high-throughput single-cell sequencing of convalescent patients' B cells. *Cell* 182, 73–84.e16 (2020). doi:10.1016/j.cell.2020.05.025 Medline
- D. F. Robbiani, C. Gaebler, F. Muecksch, J. C. C. Lorenzi, Z. Wang, A. Cho, M. Agudelo, C. O. Barnes, A. Gazumyan, S. Finkin, T. Hägglöf, T. Y. Oliveira, C. Viant, A. Hurley, H.-H. Hoffmann, K. G. Millard, R. G. Kost, M. Cipolla, K. Gordon, F. Bianchini, S. T. Chen, V. Ramos, R. Patel, J. Dizon, I. Shimeliovich, P. Mendoza, H. Hartweger, L. Nogueira, M. Pack, J. Horowitz, F. Schmidt, Y. Weisblum, E. Michailidis, A. W. Ashbrook, E. Waltari, J. E. Pak, K. E. Huey-Tubman, N. Koranda, P. R. Hoffman, A. P. West Jr., C. M. Rice, T. Hatzioannou, P. J. Bjorkman, P. D. Bieniasz, M. Caskey, M. C. Nussenzweig, Convergent antibody responses to SARS-CoV-2 in convalescent individuals. *Nature* 584, 437–442 (2020). doi:10.1038/s41586-020-2456-9 Medline
- C. O. Barnes, A. P. West Jr., K. E. Huey-Tubman, M. A. G. Hoffmann, N. G. Sharaf, P. R. Hoffman, N. Koranda, H. B. Gristick, C. Gaebler, F. Muecksch, J. C. C. Lorenzi, S. Finkin, T. Hägglöf, A. Hurley, K. G. Millard, Y. Weisblum, F. Schmidt, T. Hatzioannou, P. D. Bieniasz, M. Caskey, D. F. Robbiani, M. C. Nussenzweig, P. J. Bjorkman, Structures of human antibodies bound to SARS-CoV-2 spike reveal common epitopes and recurrent features of antibodies. *Cell* 182, 828–842.e16 (2020). doi:10.1016/j.cell.2020.06.025 Medline
- J. Kreye, S. M. Reinke, H.-C. Kornau, E. Sánchez-Sendin, V. M. Corman, H. Liu, M. Yuan, N. C. Wu, X. Zhu, C. D. Lee, J. Trimpert, M. Höltje, K. Dietert, L. Stöffler, N. von Wardenburg, S. van Hoof, M. A. Homeyer, J. Hoffmann, A. Abdelgawad, A. D. Gruber, L. D. Bertzbach, D. Vladimirova, L. Y. Li, P. C. Barthel, K. Skriner, A. C. Hocke, S. Hippenstiel, M. Witzenrath, N. Suttorp, F. Kurth, C. Franke, M. Endres, D. Schmitz, L. M. Jeworowski, A. Richter, M. L. Schmidt, T. Schwarz, M. A. Müller, C. Drosten, D. Wendisch, L. E. Sander, N. Osterrieder, I. A. Wilson, H. Prüss, A therapeutic non-self-reactive SARS-CoV-2 antibody protects from lung pathology in a COVID-19 hamster model. *Cell* 183, 1058–1069.e19 (2020). doi:10.1016/j.cell.2020.09.049 Medline
- B. Ju, Q. Zhang, J. Ge, R. Wang, J. Sun, X. Ge, J. Yu, S. Shan, B. Zhou, S. Song, X. Tang, J. Yu, J. Lan, J. Yuan, H. Wang, J. Zhao, S. Zhang, Y. Wang, X. Shi, L. Liu, J. Zhao, X. Wang, Z. Zhang, L. Zhang, Human neutralizing antibodies elicited by SARS-CoV-2 infection. *Nature* 584, 115–119 (2020). doi:10.1038/s41586-020-2380-z Medline
- D. Pinto, Y.-J. Park, M. Beltramello, A. C. Walls, M. A. Tortorici, S. Bianchi, S. Jaconi, K. Culap, F. Zatta, A. De Marco, A. Peter, B. Guarino, R. Spreafico, E. Cameroni, J. B. Case, R. E. Chen, C. Havenar-Daughton, G. Snell, A. Telenti, H. W. Virgin, A. Lanzavecchia, M. S. Diamond, K. Fink, D. Veesler, D. Corti, Cross-

- neutralization of SARS-CoV-2 by a human monoclonal SARS-CoV antibody. *Nature* **583**, 290–295 (2020). doi:10.1038/s41586-020-2349-y Medline
20. P. J. M. Brouwer, T. G. Caniels, K. van der Straten, J. L. Snitselaar, Y. Aldon, S. Bangaru, J. L. Torres, N. M. A. Okba, M. Claireaux, G. Kerster, A. E. H. Bentlage, M. M. van Haaren, D. Guerra, J. A. Burger, E. E. Schermer, K. D. Verheul, N. van der Velde, A. van der Kooi, J. van Schooten, M. J. van Breemen, T. P. L. Bijl, K. Sliepen, A. Aartse, R. Derkink, I. Bontjer, N. A. Kootstra, W. J. Wiersinga, G. Vidarsson, B. L. Haagmans, A. B. Ward, G. J. de Bree, R. W. Sanders, M. J. van Gils, Potent neutralizing antibodies from COVID-19 patients define multiple targets of vulnerability. *Science* **369**, 643–650 (2020). doi:10.1126/science.abc5902 Medline
21. Y. Wu, F. Wang, C. Shen, W. Peng, D. Li, C. Zhao, Z. Li, S. Li, Y. Bi, Y. Yang, Y. Gong, H. Xiao, Z. Fan, S. Tan, G. Wu, W. Tan, X. Lu, C. Fan, Q. Wang, Y. Liu, C. Zhang, J. Qi, G. F. Gao, F. Gao, L. Liu, A noncompeting pair of human neutralizing antibodies block COVID-19 virus binding to its receptor ACE2. *Science* **368**, 1274–1278 (2020). doi:10.1126/science.abc2241 Medline
22. X. Chi, R. Yan, J. Zhang, G. Zhang, Y. Zhang, M. Hao, Z. Zhang, P. Fan, Y. Dong, Y. Yang, Z. Chen, Y. Guo, J. Zhang, Y. Li, X. Song, Y. Chen, L. Xia, L. Fu, L. Hou, J. Xu, C. Yu, J. Li, Q. Zhou, W. Chen, A neutralizing human antibody binds to the N-terminal domain of the Spike protein of SARS-CoV-2. *Science* **369**, 650–655 (2020). doi:10.1126/science.abc6952 Medline
23. E. Seydoux, L. J. Homad, A. J. MacCamy, K. R. Parks, N. K. Hurlburt, M. F. Jennewein, N. R. Akins, A. B. Stuart, Y.-H. Wan, J. Feng, R. E. Whaley, S. Singh, M. Boeckh, K. W. Cohen, M. J. McElrath, J. A. Englund, H. Y. Chu, M. Pancera, A. T. McGuire, L. Stamatatos, Analysis of a SARS-CoV-2-infected individual reveals development of potent neutralizing antibodies with limited somatic mutation. *Immunity* **53**, 98–105.e5 (2020). doi:10.1016/j.immuni.2020.06.001 Medline
24. R. Shi, C. Shan, X. Duan, Z. Chen, P. Liu, J. Song, T. Song, X. Bi, C. Han, L. Wu, G. Gao, X. Hu, Y. Zhang, Z. Tong, W. Huang, W. J. Liu, G. Wu, B. Zhang, L. Wang, J. Qi, H. Feng, F.-S. Wang, Q. Wang, G. F. Gao, Z. Yuan, J. Yan, A human neutralizing antibody targets the receptor-binding site of SARS-CoV-2. *Nature* **584**, 120–124 (2020). doi:10.1038/s41586-020-2381-y Medline
25. X. Han, Y. Wang, S. Li, C. Hu, T. Li, C. Gu, K. Wang, M. Shen, J. Wang, J. Hu, R. Wu, S. Mu, F. Gong, Q. Chen, F. Gao, J. Huang, Y. Long, F. Luo, S. Song, S. Long, Y. Hao, L. Li, Y. Wu, W. Xu, X. Cai, Q. Gao, G. Zhang, C. He, K. Deng, L. Du, Y. Nai, W. Wang, Y. Xie, D. Qu, A. Huang, N. Tang, A. Jin, A rapid and efficient screening system for neutralizing antibodies and its application for SARS-CoV-2. *Front. Immunol.* **12**, 653189 (2021). doi:10.3389/fimmu.2021.653189 Medline
26. S. J. Zost, P. Gilchuk, R. E. Chen, J. B. Case, J. X. Reidy, A. Trivette, R. S. Nargi, R. E. Sutton, N. Suryadevara, E. C. Chen, E. Binshtein, S. Shrihari, M. Ostrowski, H. Y. Chu, J. E. Didier, K. W. MacRenaris, T. Jones, S. Day, L. Myers, F. Eun-Hyung Lee, D. C. Nguyen, I. Sanz, D. R. Martinez, P. W. Rothlauf, L.-M. Bloyet, S. P. J. Whelan, R. S. Baric, L. B. Thackray, M. S. Diamond, R. H. Carnahan, J. E. Crowe Jr., Rapid isolation and profiling of a diverse panel of human monoclonal antibodies targeting the SARS-CoV-2 spike protein. *Nat. Med.* **26**, 1422–1427 (2020). doi:10.1038/s41591-020-0998-x Medline
27. L. Liu, P. Wang, M. S. Nair, J. Yu, M. Rapp, Q. Wang, Y. Luo, J. F.-W. Chan, V. Sahi, A. Figueroa, X. V. Guo, G. Cerutti, J. Bimela, J. Gorman, T. Zhou, Z. Chen, K.-Y. Yuen, P. D. Kwong, J. G. Sodroski, M. T. Yin, Z. Sheng, Y. Huang, L. Shapiro, D. D. Ho, Potent neutralizing antibodies against multiple epitopes on SARS-CoV-2 spike. *Nature* **584**, 450–456 (2020). doi:10.1038/s41586-020-2571-7 Medline
28. J. Hansen, A. Baum, K. E. Pascal, V. Russo, S. Giordano, E. Wloga, B. O. Fulton, Y. Yan, K. Koon, K. Patel, K. M. Chung, A. Hermann, E. Ullman, J. Cruz, A. Rafique, T. Huang, J. Fairhurst, C. Libertiny, M. Malbec, W. Y. Lee, R. Welsh, G. Farr, S. Pennington, D. Deshpande, J. Cheng, A. Watty, P. Bouffard, R. Babbs, N. Levenkova, C. Chen, B. Zhang, A. Romero Hernandez, K. Saotome, Y. Zhou, M. Franklin, S. Sivapalasingam, D. C. Lye, S. Weston, J. Logue, R. Haupt, M. Frieman, G. Chen, W. Olson, A. J. Murphy, N. Stahl, G. D. Yancopoulos, C. A. Kyriatsous, Studies in humanized mice and convalescent humans yield a SARS-CoV-2 antibody cocktail. *Science* **369**, 1010–1014 (2020). doi:10.1126/science.abd0827 Medline
29. C. Kreer, M. Zehner, T. Weber, M. S. Ercanoglu, L. Gieselmann, C. Rohde, S. Halwe, M. Korenkov, P. Schommers, K. Vanshylla, V. Di Cristanziano, H. Janicki, R. Brinker, A. Ashurov, V. Krähling, A. Kupke, H. Cohen-Dvashi, M. Koch, J. M. Eckert, S. Lederer, N. Pfeifer, T. Wolf, M. J. G. T. Vehreschild, C. Wendtner, R. Diskin, H. Gruell, S. Becker, F. Klein, Longitudinal isolation of potent near-germline SARS-CoV-2-neutralizing antibodies from COVID-19 patients. *Cell* **182**, 843–854.e12 (2020). doi:10.1016/j.cell.2020.06.044 Medline
30. M. A. Tortorici, M. Beltramello, F. A. Lempp, D. Pinto, H. V. Dang, L. E. Rosen, M. McCallum, J. Bowen, A. Minola, S. Jaconi, F. Zatta, A. De Marco, B. Guarino, S. Bianchi, E. J. Lauron, H. Tucker, J. Zhou, A. Peter, C. Havenar-Daughton, J. A. Wojcechowskyj, J. B. Case, R. E. Chen, H. Kaiser, M. Montiel-Ruiz, M. Meury, N. Czudnochowski, R. Spreafico, J. Dillen, C. Ng, N. Sprugasci, K. Culap, F. Benigni, R. Abdelnabi, S. C. Foo, M. A. Schmid, E. Cameroni, A. Riva, A. Gabrieli, M. Galli, M. S. Pizzuto, J. Neyts, M. S. Diamond, H. W. Virgin, G. Snell, D. Corti, K. Fink, D. Veesler, Ultrapotent human antibodies protect against SARS-CoV-2 challenge via multiple mechanisms. *Science* **370**, 950–957 (2020). doi:10.1126/science.abe3354 Medline
31. L. Piccoli, Y.-J. Park, M. A. Tortorici, N. Czudnochowski, A. C. Walls, M. Beltramello, C. Silacci-Fregnini, D. Pinto, L. E. Rosen, J. E. Bowen, O. J. Acton, S. Jaconi, B. Guarino, A. Minola, F. Zatta, N. Sprugasci, J. Bassi, A. Peter, A. De Marco, J. C. Nix, F. Mele, S. Jovic, B. F. Rodriguez, S. V. Gupta, F. Jin, G. Piumatti, G. Lo Presti, A. F. Pellanda, M. Biggiogero, M. Tarkowski, M. S. Pizzuto, E. Cameroni, C. Havenar-Daughton, M. Smithey, D. Hong, V. Lepori, E. Albanese, A. Ceschi, E. Bernasconi, L. Elzi, P. Ferrari, C. Garzoni, A. Riva, G. Snell, F. Sallusto, K. Fink, H. W. Virgin, A. Lanzavecchia, D. Corti, D. Veesler, Mapping neutralizing and immunodominant sites on the SARS-CoV-2 spike receptor-binding domain by structure-guided high-resolution serology. *Cell* **183**, 1024–1042.e21 (2020). doi:10.1016/j.cell.2020.09.037 Medline
32. S. A. Clark, L. E. Clark, J. Pan, A. Coscia, L. G. A. McKay, S. Shankar, R. I. Johnson, V. Brusic, M. C. Choudhary, J. Regan, J. Z. Li, A. Griffiths, J. Abraham, SARS-CoV-2 evolution in an immunocompromised host reveals shared neutralization escape mechanisms. *Cell* **184**, 2605–2617.e18 (2021). doi:10.1016/j.cell.2021.03.027 Medline
33. M. Mor, M. Werbner, J. Alter, M. Safra, E. Chomsky, J. C. Lee, S. Hada-Neeman, K. Polonsky, C. J. Nowell, A. E. Clark, A. Roitburd-Berman, N. Ben-Shalom, M. Navon, D. Rafael, H. Sharim, E. Kiner, E. R. Griffis, J. M. Gershoni, O. Kobiler, S. L. Leibel, O. Zimhony, A. F. Carlin, G. Yaari, M. Dessau, M. Gal-Tanamy, D. Hagin, B. A. Croker, N. T. Freund, Multi-clonal SARS-CoV-2 neutralization by antibodies isolated from severe COVID-19 convalescent donors. *PLOS Pathog.* **17**, e1009165 (2021). doi:10.1371/journal.ppat.1009165 Medline
34. R. Babb et al. (Regeneron Pharmaceuticals Inc.), U.S. Patent 10787501 (2020); <https://uspto.report/patent/grant/10.787.501>.
35. M. Yuan, N. C. Wu, X. Zhu, C. D. Lee, R. T. Y. So, H. Lv, C. K. P. Mok, I. A. Wilson, A highly conserved cryptic epitope in the receptor binding domains of SARS-CoV-2 and SARS-CoV. *Science* **368**, 630–633 (2020). doi:10.1126/science.abb7269 Medline
36. N. K. Hurlburt, E. Seydoux, Y.-H. Wan, V. V. Edara, A. B. Stuart, J. Feng, M. S. Suthar, A. T. McGuire, L. Stamatatos, M. Pancera, Structural basis for potent neutralization of SARS-CoV-2 and role of antibody affinity maturation. *Nat. Commun.* **11**, 5413 (2020). doi:10.1038/s41467-020-19231-9 Medline
37. T. Noy-Porat, E. Makdasi, R. Alcalay, A. Mechaly, Y. Levy, A. Bercovich-Kinori, A. Zauberan, H. Tamir, Y. Yahalom-Ronen, M. Israeli, E. Epstein, H. Achdout, S. Melamed, T. Chitlaru, S. Weiss, E. Peretz, O. Rosen, N. Paran, S. Yitzhaki, S. C. Shapira, T. Israely, O. Mazor, R. Rosenfeld, A panel of human neutralizing mAbs targeting SARS-CoV-2 spike at multiple epitopes. *Nat. Commun.* **11**, 4303 (2020). doi:10.1038/s41467-020-18159-4 Medline
38. S. Du, Y. Cao, Q. Zhu, P. Yu, F. Qi, G. Wang, X. Du, L. Bao, W. Deng, H. Zhu, J. Liu, J. Nie, Y. Zheng, H. Liang, R. Liu, S. Gong, H. Xu, A. Yisimayi, Q. Lv, B. Wang, R. He, Y. Han, W. Zhao, Y. Bai, Y. Qu, X. Gao, C. Ji, Q. Wang, N. Gao, W. Huang, Y. Wang, X. S. Xie, X. D. Su, J. Xiao, C. Qin, Structurally resolved SARS-CoV-2 antibody shows high efficacy in severely infected hamsters and provides a potent cocktail pairing strategy. *Cell* **183**, 1013–1023.e13 (2020). doi:10.1016/j.cell.2020.09.035 Medline

39. Y. Zhou, Z. Liu, S. Li, W. Xu, Q. Zhang, I. T. Silva, C. Li, Y. Wu, Q. Jiang, Z. Liu, Q. Wang, Y. Guo, J. Wu, C. Gu, X. Cai, D. Qu, C. T. Mayer, X. Wang, S. Jiang, T. Ying, Z. Yuan, Y. Xie, Y. Wen, L. Lu, Q. Wang. Enhancement versus neutralization by SARS-CoV-2 antibodies from a convalescent donor associates with distinct epitopes on the RBD. *Cell Rep.* **34**, 108699 (2021). [doi:10.1016/j.celrep.2021.108699](https://doi.org/10.1016/j.celrep.2021.108699) Medline
40. A. R. Shiakolas, K. J. Kramer, D. Wrapp, S. I. Richardson, A. Schäfer, S. Wall, N. Wang, K. Janowska, K. A. Pilewski, R. Venkat, R. Parks, N. P. Manamela, N. Raju, E. F. Fechter, C. M. Holt, N. Suryadevara, R. E. Chen, D. R. Martinez, R. S. Nargi, R. E. Sutton, J. E. Ledgerwood, B. S. Graham, M. S. Diamond, B. F. Haynes, P. Acharya, R. H. Carnahan, J. E. Crowe, R. S. Baric, L. Morris, J. S. McLellan, I. S. Georgiev, Cross-reactive coronavirus antibodies with diverse epitope specificities and extra-neutralization functions. bioRxiv [414748](https://doi.org/10.1101/414748) [preprint]. 20 December 2020.
41. D. Li, R. J. Edwards, K. Manne, D. R. Martinez, A. Schäfer, S. M. Alam, K. Wiehe, X. Lu, R. Parks, L. L. Sutherland, T. H. Oguin, C. McDanal, L. G. Perez, K. Mansouri, S. M. C. Gobell, K. Janowska, V. Stalls, M. Kopp, F. Cai, E. Lee, A. Foulger, G. E. Hernandez, A. Sanzone, K. Tilahun, C. Jiang, L. V. Tse, K. W. Bock, M. Minai, B. M. Nagata, K. Cronin, V. Gee-Lai, M. Deyton, M. Barr, T. Von Holle, A. N. Macintyre, E. Stover, J. Feldman, B. M. Hauser, T. M. Caradonna, T. D. Scobey, M. A. Moody, D. W. Cain, C. T. DeMarco, T. N. Denny, C. W. Woods, E. W. Petzold, A. G. Schmidt, I. T. Teng, T. Zhou, P. D. Kwong, J. R. Mascola, B. S. Graham, I. N. Moore, R. Seder, H. Andersen, M. G. Lewis, D. C. Montefiori, G. D. Sempowski, R. S. Baric, P. Acharya, B. F. Haynes, K. O. Saunders, The functions of SARS-CoV-2 neutralizing and infection-enhancing antibodies in vitro and in mice and nonhuman primates. bioRxiv [424729](https://doi.org/10.1101/424729) [preprint]. 2 January 2021.
42. B. B. Banach, G. Cerutti, A. S. Fahad, C. H. Shen, M. O. de Souza, P. S. Katsamba, Y. Tsibovsky, P. Wang, M. S. Nair, Y. Huang, I. M. F. Urdániz, P. J. Steiner, M. Gutiérrez-González, L. Liu, S. N. López Acevedo, A. Nazzari, J. R. Wolfe, Y. Luo, A. S. Olia, I. T. Teng, J. Yu, T. Zhou, E. R. Reddem, J. Bimela, X. Pan, B. Madan, A. D. Laflin, R. Nimrania, K. T. Yuen, T. A. Whitehead, D. D. Ho, P. D. Kwong, L. Shapiro, B. J. DeKosky, Paired heavy and light chain signatures contribute to potent SARS-CoV-2 neutralization in public antibody responses. bioRxiv [424987](https://doi.org/10.1101/424987) [preprint]. 3 January 2021.
43. G. Bullen et al., Deep mining of early antibody response in COVID-19 patients yields potent neutralisers and reveals high level of convergence. bioRxiv [424711](https://doi.org/10.1101/424711) [preprint]. 29 December 2020.
44. J. Wan, S. Xing, L. Ding, Y. Wang, C. Gu, Y. Wu, B. Rong, C. Li, S. Wang, K. Chen, C. He, D. Zhu, S. Yuan, C. Qiu, C. Zhao, L. Nie, Z. Gao, J. Jiao, X. Zhang, X. Wang, T. Ying, H. Wang, Y. Xie, Y. Lu, J. Xu, F. Lan, Human-IgG-neutralizing monoclonal antibodies block the SARS-CoV-2 infection. *Cell Rep.* **32**, 107918 (2020). [doi:10.1016/j.celrep.2020.107918](https://doi.org/10.1016/j.celrep.2020.107918) Medline
45. Y. Weisblum, F. Schmidt, F. Zhang, J. DaSilva, D. Poston, J. C. C. Lorenzi, F. Muecksch, M. Rutkowska, H.-H. Hoffmann, E. Michailidis, C. Gaebler, M. Agudelo, A. Cho, Z. Wang, A. Gazumyan, M. Cipolla, L. Luchsinger, C. D. Hillyer, M. Caskey, D. F. Robbiani, C. M. Rice, M. C. Nussenzweig, T. Hatzioannou, P. D. Bieniasz, Escape from neutralizing antibodies by SARS-CoV-2 spike protein variants. *eLife* **9**, e61312 (2020). [doi:10.7554/elife.61312](https://doi.org/10.7554/elife.61312) Medline
46. A. J. Greaney, T. N. Starr, P. Gilchuk, S. J. Zost, E. Binshtein, A. N. Loes, S. K. Hilton, J. Huddleston, R. Eguia, K. H. D. Crawford, A. S. Dingens, R. S. Nargi, R. E. Sutton, N. Suryadevara, P. W. Rothlauf, Z. Liu, S. P. J. Whelan, R. H. Carnahan, J. E. Crowe Jr., J. D. Bloom, Complete mapping of mutations to the SARS-CoV-2 spike receptor-binding domain that escape antibody recognition. *Cell Host Microbe* **29**, 44–57.e9 (2021). [doi:10.1016/j.chom.2020.11.007](https://doi.org/10.1016/j.chom.2020.11.007) Medline
47. E. Andreano, G. Piccini, D. Licastro, L. Casalino, N. V. Johnson, I. Paciello, S. D. Monego, E. Pantano, N. Manganaro, A. Manenti, R. Manna, E. Casa, I. Hyseni, L. Benincasa, E. Montomoli, R. E. Amaro, J. S. McLellan, R. Rappuoli, SARS-CoV-2 escape in vitro from a highly neutralizing COVID-19 convalescent plasma. bioRxiv [424451](https://doi.org/10.1101/424451) [preprint]. 28 December 2020.
48. C. K. Wibmer, F. Ayres, T. Hermanus, M. Madzhivhandila, P. Kgagudi, B. Oosthuysen, B. E. Lambson, T. de Oliveira, M. Vermeulen, K. van der Berg, T. Rossouw, M. Boswell, V. Ueckermann, S. Meiring, A. von Gottberg, C. Cohen, L. Morris, J. N. Bhiman, P. L. Moore, SARS-CoV-2 501Y.V2 escapes neutralization by South African COVID-19 donor plasma. *Nat. Med.* **27**, 622–625 (2021). [doi:10.1038/s41591-021-01285-x](https://doi.org/10.1038/s41591-021-01285-x) Medline
49. A. J. Greaney, A. N. Loes, K. H. D. Crawford, T. N. Starr, K. D. Malone, H. Y. Chu, J. D. Bloom, Comprehensive mapping of mutations in the SARS-CoV-2 receptor-binding domain that affect recognition by polyclonal human plasma antibodies. *Cell Host Microbe* **29**, 463–476.e6 (2021). [doi:10.1016/j.chom.2021.02.003](https://doi.org/10.1016/j.chom.2021.02.003) Medline
50. Z. Wang, F. Schmidt, Y. Weisblum, F. Muecksch, C. O. Barnes, S. Finkin, D. Schaefer-Babajew, M. Cipolla, C. Gaebler, J. A. Lieberman, T. Y. Oliveira, Z. Yang, M. E. Abernathy, K. E. Huey-Tubman, A. Hurley, M. Turroja, K. A. West, K. Gordon, K. G. Millard, V. Ramos, J. Da Silva, J. Xu, R. A. Colbert, R. Patel, J. Dizon, C. Unson-O'Brien, I. Shimeliovich, A. Gazumyan, M. Caskey, P. J. Bjorkman, R. Casellas, T. Hatzioannou, P. D. Bieniasz, M. C. Nussenzweig, mRNA vaccine-elicited antibodies to SARS-CoV-2 and circulating variants. *Nature* **592**, 616–622 (2021). [doi:10.1038/s41586-021-03324-6](https://doi.org/10.1038/s41586-021-03324-6) Medline
51. L. Stamatatos, J. Czartoski, Y.-H. Wan, L. J. Homad, V. Rubin, H. Glantz, M. Neradilek, E. Seydoux, M. F. Jennewein, A. J. MacCamy, J. Feng, G. Mize, S. C. De Rosa, A. Finzi, M. P. Lemos, K. W. Cohen, Z. Moodie, M. J. McElrath, A. T. McGuire, mRNA vaccination boosts cross-variant neutralizing antibodies elicited by SARS-CoV-2 infection. *Science* [abg9175](https://doi.org/10.1126/science.abg9175) (2021). [doi:10.1126/science.abg9175](https://doi.org/10.1126/science.abg9175) Medline
52. L. Wang, T. Zhou, Y. Zhang, E. S. Yang, C. A. Schramm, W. Shi, A. Pegu, O. K. Oloniyi, A. Ransier, S. Darko, S. R. Narpala, C. Hatcher, D. R. Martinez, Y. Tsibovsky, E. Phung, O. M. Abiona, E. M. Cale, L. A. Chang, K. S. Corbett, A. T. DiPiazza, I. J. Gordon, K. Leung, T. Liu, R. D. Mason, A. Nazzari, L. Novik, A. S. Olia, T. Stephens, C. D. Stringham, C. A. Talana, I. T. Teng, D. Wagner, A. T. Wedge, B. Zhang, M. Roederer, J. E. Ledgerwood, T. J. Rockwardt, M. R. Gaudinski, R. S. Baric, B. S. Graham, A. B. McDermott, D. C. Douek, P. D. Kwong, J. R. Mascola, N. J. Sullivan, J. Misasi, Antibodies with potent and broad neutralizing activity against antigenically diverse and highly transmissible SARS-CoV-2 variants. bioRxiv [432969](https://doi.org/10.1101/432969) [preprint]. 26 February 2021.
53. X. Xie, Y. Liu, J. Liu, X. Zhang, J. Zou, C. R. Fontes-Garfias, H. Xia, K. A. Swanson, M. Cutler, D. Cooper, V. D. Menachery, S. C. Weaver, P. R. Dormitzer, P.-Y. Shi, Neutralization of SARS-CoV-2 spike 69/70 deletion, E484K and N501Y variants by BNT162b2 vaccine-elicited sera. *Nat. Med.* **27**, 620–621 (2021). [doi:10.1038/s41591-021-01270-4](https://doi.org/10.1038/s41591-021-01270-4) Medline
54. D. A. Collier, A. De Marco, I. A. T. M. Ferreira, B. Meng, R. P. Datir, A. C. Walls, S. A. Kemp, J. Bassi, D. Pinto, C. Silacci-Fregni, S. Bianchi, M. A. Tortorici, J. Bowen, K. Culap, S. Jaconi, E. Cameroni, G. Snell, M. S. Pizzuto, A. F. Pellanda, C. Garzoni, A. Riva, A. Elmer, N. Kingston, B. Graves, L. E. McCoy, K. G. C. Smith, J. R. Bradley, N. Temperton, L. Cerón-Gutierrez, G. Barcenas-Morales, W. Harvey, H. W. Virgin, A. Lanzavecchia, L. Piccoli, R. Doffinger, M. Wills, D. Veesler, D. Corti, R. K. Gupta, CITIID-NIHR BioResource COVID-19 Collaboration, COVID-19 Genomics UK (COG-UK) Consortium, Sensitivity of SARS-CoV-2 B.1.1.7 to mRNA vaccine-elicited antibodies. *Nature* **593**, 136–141 (2021). [doi:10.1038/s41586-021-03412-7](https://doi.org/10.1038/s41586-021-03412-7) Medline
55. W. F. Garcia-Beltran, E. C. Lam, K. St. Denis, A. D. Nitido, Z. H. Garcia, B. M. Hauser, J. Feldman, M. N. Pavlovic, D. J. Gregory, M. C. Poznansky, A. Sigal, A. G. Schmidt, A. J. Lafrate, V. Naranhai, A. B. Balazs, Multiple SARS-CoV-2 variants escape neutralization by vaccine-induced humoral immunity. *Cell* **184**, 2372–2383.e9 (2021). [doi:10.1016/j.cell.2021.03.013](https://doi.org/10.1016/j.cell.2021.03.013) Medline
56. V. Shinde et al., Efficacy of the NVX-CoV2373 Covid-19 vaccine against the B.1.351 variant. *N. Engl. J. Med.* **384**, 1899–1909 (2021). [doi:10.1056/NEJMoa2103055](https://doi.org/10.1056/NEJMoa2103055)
57. R. E. Chen, X. Zhang, J. B. Case, E. S. Winkler, Y. Liu, L. A. VanBlargan, J. Liu, J. M. Errico, X. Xie, N. Suryadevara, P. Gilchuk, S. J. Zost, S. Tahan, L. Droit, J. S. Turner, W. Kim, A. J. Schmitz, M. Thapa, D. Wang, A. C. M. Boon, R. M. Presti, J. A. O'Halloran, A. H. J. Kim, P. Deepak, D. Pinto, D. H. Fremont, J. E. Crowe Jr., D. Corti, H. W. Virgin, A. H. Ellebedy, P.-Y. Shi, M. S. Diamond, Resistance of SARS-CoV-2 variants to neutralization by monoclonal and serum-derived polyclonal antibodies. *Nat. Med.* **27**, 717–726 (2021). [doi:10.1038/s41591-021-01294-w](https://doi.org/10.1038/s41591-021-01294-w)

Medline

58. X. Shen, H. Tang, C. McDanal, K. Wagh, W. Fischer, J. Theiler, H. Yoon, D. Li, B. F. Haynes, K. O. Sanders, S. Gnanakaran, N. Hengartner, R. Pajon, G. Smith, G. M. Glenn, B. Korber, D. C. Montefiori, SARS-CoV-2 variant B.1.1.7 is susceptible to neutralizing antibodies elicited by ancestral spike vaccines. *Cell Host Microbe* **29**, 529–539.e3 (2021). doi:10.1016/j.chom.2021.03.002 Medline
59. S. Cele, I. Gazy, L. Jackson, S.-H. Hwa, H. Tegally, G. Lustig, J. Giandhari, S. Pillay, E. Wilkinson, Y. Naidoo, F. Karim, Y. Ganga, K. Khan, M. Bernstein, A. B. Balazs, B. I. Gosnell, W. Hanekom, M. S. Moosa, R. J. Lessells, T. de Oliveira, A. Sigal, Network for Genomic Surveillance in South Africa, COMMIT-KZN Team, Escape of SARS-CoV-2 501Y.V2 from neutralization by convalescent plasma. *Nature* **593**, 142–146 (2021). doi:10.1038/s41586-021-03471-w Medline
60. V. V. Edara, C. Norwood, K. Floyd, L. Lai, M. E. Davis-Gardner, W. H. Hudson, G. Mantus, L. E. Nyhoff, M. W. Adelman, R. Fineman, S. Patel, R. Byram, D. N. Gomes, G. Michael, H. Abdullahi, N. Beydoun, B. Panganiban, N. McNair, K. Hellmeister, J. Pitts, J. Winters, J. Kleinhenz, J. Usher, J. B. O'Keefe, A. Piantadosi, J. J. Waggoner, A. Babiker, D. S. Stephens, E. J. Anderson, S. Edupuganti, N. Rouphael, R. Ahmed, J. Wrammert, M. S. Suthar, Infection- and vaccine-induced antibody binding and neutralization of the B.1.351 SARS-CoV-2 variant. *Cell Host Microbe* **29**, 516–521.e3 (2021). doi:10.1016/j.chom.2021.03.009 Medline
61. J. Hu, P. Peng, K. Wang, L. Fang, F. Y. Luo, A. S. Jin, B. Z. Liu, N. Tang, A. L. Huang, Emerging SARS-CoV-2 variants reduce neutralization sensitivity to convalescent sera and monoclonal antibodies. *Cell. Mol. Immunol.* **18**, 1061–1063 (2021). doi:10.1038/s41423-021-00648-1 Medline
62. R. Wang et al., SARS-CoV-2 variants resist antibody neutralization and broaden host ACE2 usage. bioRxiv **434497** [preprint]. 15 March 2021.
63. W. Dejnirattisai, D. Zhou, P. Supasa, C. Liu, A. J. Mentzer, H. M. Ginn, Y. Zhao, H. M. E. Duyvesteyn, A. Tuekprakhon, R. Nutalai, B. Wang, C. López-Camacho, J. Slon-Campos, T. S. Walter, D. Skelly, S. A. Costa Clemens, F. G. Naveca, V. Nascimento, F. Nascimento, C. Fernandes da Costa, P. C. Resende, A. Pauvolid-Correia, M. M. Siqueira, C. Dold, R. Levin, T. Dong, A. J. Pollard, J. C. Knight, D. Crook, T. Lambe, E. Clutterbuck, S. Bibi, A. Flaxman, M. Bittaye, S. Belij-Rammerstorfer, S. C. Gilbert, M. W. Carroll, P. Klenerman, E. Barnes, S. J. Dunachie, N. G. Paterson, M. A. Williams, D. R. Hall, R. J. G. Hulswit, T. A. Bowden, E. E. Fry, J. Mongkolsapaya, J. Ren, D. I. Stuart, G. R. Screaton, Antibody evasion by the P.1 strain of SARS-CoV-2. *Cell* **S0092-8674(21)00428-1** (2021). doi:10.1016/j.cell.2021.03.055 Medline
64. M. Hoffmann, P. Arora, R. Groß, A. Seidel, B. F. Hörmich, A. S. Hahn, N. Krüger, L. Graichen, H. Hofmann-Winkler, A. Kempf, M. S. Winkler, S. Schulz, H.-M. Jack, B. Jahrsdörfer, H. Schrezenmeier, M. Müller, A. Kleger, J. Münch, S. Pöhlmann, SARS-CoV-2 variants B.1.351 and P.1 escape from neutralizing antibodies. *Cell* **184**, 2384–2393.e12 (2021). doi:10.1016/j.cell.2021.03.036 Medline
65. D. Planas, T. Bruel, L. Grzelak, F. Guivel-Benhassine, I. Staropoli, F. Porrot, C. Planchais, J. Buchrieser, M. M. Rajah, E. Bishop, M. Albert, F. Donati, M. Prot, S. Behillil, V. Enouf, M. Maquart, M. Smati-Lafarge, E. Varon, F. Schortgen, L. Yahyaoui, M. Gonzalez, J. De Sèze, H. Pétré, D. Veyer, A. Sève, E. Simon-Lorière, S. Fafi-Kremer, K. Stefic, H. Mouquet, L. Hocqueloux, S. van der Werf, T. Prazuck, O. Schwartz, Sensitivity of infectious SARS-CoV-2 B.1.1.7 and B.1.351 variants to neutralizing antibodies. *Nat. Med.* **27**, 917–924 (2021). doi:10.1038/s41591-021-01318-5 Medline
66. P. Wang, M. S. Nair, L. Liu, S. Iketani, Y. Luo, Y. Guo, M. Wang, J. Yu, B. Zhang, P. D. Kwong, B. S. Graham, J. R. Mascola, J. Y. Chang, M. T. Yin, M. Sobieszczky, C. A. Kyratsous, L. Shapiro, Z. Sheng, Y. Huang, D. D. Ho, Antibody resistance of SARS-CoV-2 variants B.1.351 and B.1.1.7. *Nature* **593**, 130–135 (2021). doi:10.1038/s41586-021-03398-2 Medline
67. P. Wang, R. G. Casner, M. S. Nair, M. Wang, J. Yu, G. Cerutti, L. Liu, P. D. Kwong, Y. Huang, L. Shapiro, D. D. Ho, Increased resistance of SARS-CoV-2 variant P.1 to antibody neutralization. bioRxiv **433466** [preprint]. 2 March 2021.
68. D. Zhou, W. Dejnirattisai, P. Supasa, C. Liu, A. J. Mentzer, H. M. Ginn, Y. Zhao, H. M. E. Duyvesteyn, A. Tuekprakhon, R. Nutalai, B. Wang, G. C. Paesen, C. Lopez-Camacho, J. Slon-Campos, B. Hallis, N. Coombes, K. Bewley, S. Charlton, T. S. Walter, D. Skelly, S. F. Lumley, C. Dold, R. Levin, T. Dong, A. J. Pollard, J. C. Knight, D. Crook, T. Lambe, E. Clutterbuck, S. Bibi, A. Flaxman, M. Bittaye, S. Belij-Rammerstorfer, S. Gilbert, W. James, M. W. Carroll, P. Klenerman, E. Barnes, S. J. Dunachie, E. E. Fry, J. Mongkolsapaya, J. Ren, D. I. Stuart, G. R. Screaton, Evidence of escape of SARS-CoV-2 variant B.1.351 from natural and vaccine-induced sera. *Cell* **184**, 2348–2361.e6 (2021). doi:10.1016/j.cell.2021.02.037 Medline
69. G. Cerutti, M. Rapp, Y. Guo, F. Bahna, J. Jimela, E. R. Reddem, J. Yu, P. Wang, L. Liu, Y. Huang, D. D. Ho, P. D. Kwong, Z. Sheng, L. Shapiro, Structural basis for accommodation of emerging B.1.351 and B.1.1.7 variants by two potent SARS-CoV-2 neutralizing antibodies. bioRxiv **432168** [preprint]. 22 February 2021.
70. T. N. Starr, N. Czudnochowski, F. Zatta, Y. J. Park, Z. Liu, A. Addetia, D. Pinto, M. Beltramello, P. Hernandez, A. J. Greaney, R. Marzi, W. G. Glass, I. Zhang, A. S. Dingens, J. E. Bowen, J. A. Wojciechowsky, A. De Marco, L. E. Rosen, J. Zhou, M. Montiel-Ruiz, H. Kaiser, H. Tucker, M. P. Housley, J. di Julio, G. Lombardo, M. Agostini, N. Sprugasci, K. Culap, S. Jaconi, M. Meury, E. Dellota, E. Cameroni, T. I. Croll, J. C. Nix, C. Havenar-Daughton, A. Telenti, F. A. Lempp, M. S. Pizzuto, J. D. Chodera, C. M. Hebnar, S. P. J. Whelan, H. W. Virgin, D. Veesler, D. Corti, J. D. Bloom, G. Snell, Antibodies to the SARS-CoV-2 receptor-binding domain that maximize breadth and resistance to viral escape. bioRxiv **438709** [preprint]. 8 April 2021.
71. Binding and neutralization of IGHV3-66 antibodies were also abolished by K417N, as shown by (62), where IGHV3-66 antibody CB6, which binds to RBD in IGHV3-53/3-66 binding mode 1 (fig. S4A), was not able to bind or neutralize K417N and B.1.351 or P.1.
72. The epitopes have been assigned on their interaction with a single RBD. Quaternary epitopes are not considered in these assignments.
73. While the antibodies structurally characterized to date do not represent all of the antibodies in a polyclonal response, they do represent major families of antibodies that have been found in the sera of convalescent SARS-CoV-2 patients.
74. We originally referred these IGHV3-53/3-66 binding modes as "A" and "B" in (9) and (75). To distinguish from "RBS-A" and "RBS-B", these IGHV3-53/3-66 binding modes are referred to as "IGHV3-53/3-66 binding mode 1" and "2" in this study. Likewise, IGHV1-2 antibodies approach the RBD in two binding modes, which are referred as "IGHV1-2 binding mode 1" and "2". The definitions of the binding modes in these two germline-encoded antibodies differ from "class 1" and "class 2" in (10), which were defined as ACE2-blocking antibodies that bind to "up-RBD only" and to "up/down RBD", respectively.
75. N. C. Wu, M. Yuan, H. Liu, C. D. Lee, X. Zhu, S. Bangaru, J. L. Torres, T. G. Caniels, P. J. M. Brouwer, M. J. van Gils, R. W. Sanders, A. B. Ward, I. A. Wilson, An alternative binding mode of IGHV3-53 antibodies to the SARS-CoV-2 receptor binding domain. *Cell Rep.* **33**, 108274 (2020). doi:10.1016/j.celrep.2020.108274 Medline
76. S. D. Boyd, B. A. Gaëta, K. J. Jackson, A. Z. Fire, E. L. Marshall, J. D. Merker, J. M. Maniar, L. N. Zhang, B. Sahaf, C. D. Jones, B. B. Simen, B. Hanczaruk, K. D. Nguyen, K. C. Nadeau, M. Egholm, D. B. Miklos, J. L. Zehnder, A. M. Collins, Individual variation in the germline Ig gene repertoire inferred from variable region gene rearrangements. *J. Immunol.* **184**, 6986–6992 (2010). doi:10.4049/jimmunol.1000445 Medline
77. M. Rapp, Y. Guo, E. R. Reddem, J. Yu, L. Liu, P. Wang, G. Cerutti, P. Katsamba, J. S. Jimela, F. A. Bahna, S. M. Mannepalli, B. Zhang, P. D. Kwong, Y. Huang, D. D. Ho, L. Shapiro, Z. Sheng, Modular basis for potent SARS-CoV-2 neutralization by a prevalent VH1-2-derived antibody class. *Cell Rep.* **35**, 108950 (2021). doi:10.1016/j.celrep.2021.108950 Medline
78. H. Yao, Y. Sun, Y.-Q. Deng, N. Wang, Y. Tan, N.-N. Zhang, X.-F. Li, C. Kong, Y.-P. Xu, Q. Chen, T.-S. Cao, H. Zhao, X. Yan, L. Cao, Z. Lv, D. Zhu, R. Feng, N. Wu, W. Zhang, Y. Hu, K. Chen, R.-R. Zhang, Q. Lv, S. Sun, Y. Zhou, R. Yan, G. Yang, X. Sun, C. Liu, X. Lu, L. Cheng, H. Qiu, X.-Y. Huang, T. Weng, D. Shi, W. Jiang, J. Shao, L. Wang, J. Zhang, T. Jiang, G. Lang, C.-F. Qin, L. Li, X. Wang, Rational development of a human antibody cocktail that deploys multiple functions to confer Pan-SARS-CoVs protection. *Cell Res.* **31**, 25–36 (2021).

- [doi:10.1038/s41422-020-00444-y](https://doi.org/10.1038/s41422-020-00444-y) Medline
79. RBS-C antibodies CV07-270, BD-368-2, P2B-2F6, C104, and P17 are encoded by IGHV3-11, IGHV3-23, IGHV4-38-2, IGHV4-34, and IGHV3-30, respectively.
80. H. Liu, N. C. Wu, M. Yuan, S. Bangaru, J. L. Torres, T. G. Caniels, J. van Schooten, X. Zhu, C. D. Lee, P. J. M. Brouwer, M. J. van Gils, R. W. Sanders, A. B. Ward, I. A. Wilson, Cross-neutralization of a SARS-CoV-2 antibody to a functionally conserved site is mediated by avidity. *Immunity* **53**, 1272–1280.e5 (2020). [doi:10.1016/j.jimmuni.2020.10.023](https://doi.org/10.1016/j.jimmuni.2020.10.023) Medline
81. H. Liu, M. Yuan, D. Huang, S. Bangaru, F. Zhao, C. D. Lee, L. Peng, S. Barman, X. Zhu, D. Nemazee, D. R. Burton, M. J. van Gils, R. W. Sanders, H.-C. Kornau, S. M. Reincke, H. Prüss, J. Kreye, N. C. Wu, A. B. Ward, I. A. Wilson, A combination of cross-neutralizing antibodies synergizes to prevent SARS-CoV-2 and SARS-CoV pseudovirus infection. *Cell Host Microbe* **29**, 806–818.e6 (2021). [doi:10.1016/j.chom.2021.04.005](https://doi.org/10.1016/j.chom.2021.04.005) Medline
82. K. Wu, A. P. Werner, J. I. Moliva, M. Koch, A. Choi, G. B. E. Stewart-Jones, H. Bennett, S. Boyoglu-Barnum, W. Shi, B. S. Graham, A. Carfi, K. S. Corbett, R. A. Seder, D. K. Edwards, mRNA-1273 vaccine induces neutralizing antibodies against spike mutants from global SARS-CoV-2 variants. *bioRxiv* [427948](https://doi.org/10.1101/27948) [preprint]. 25 January 2021.
83. G. B. Karlsson Hedestam, R. A. M. Fouchier, S. Phogat, D. R. Burton, J. Sodroski, R. T. Wyatt, The challenges of eliciting neutralizing antibodies to HIV-1 and to influenza virus. *Nat. Rev. Microbiol.* **6**, 143–155 (2008). [doi:10.1038/nrmicro1819](https://doi.org/10.1038/nrmicro1819) Medline
84. B. Choi, M. C. Choudhary, J. Regan, J. A. Sparks, R. F. Padera, X. Qiu, I. H. Solomon, H.-H. Kuo, J. Boucau, K. Bowman, U. D. Adhikari, M. L. Winkler, A. A. Mueller, T. Y.-T. Hsu, M. Desjardins, L. R. Baden, B. T. Chan, B. D. Walker, M. Lichterfeld, M. Brigl, D. S. Kwon, S. Kanjilal, E. T. Richardson, A. H. Jonsson, G. Alter, A. K. Barczak, W. P. Hanage, X. G. Yu, G. D. Gaiha, M. S. Seaman, M. Cernadas, J. Z. Li, Persistence and evolution of SARS-CoV-2 in an immunocompromised host. *N. Engl. J. Med.* **383**, 2291–2293 (2020). [doi:10.1056/NEJMc2031364](https://doi.org/10.1056/NEJMc2031364) Medline
85. K. Wu, A. P. Werner, M. Koch, A. Choi, E. Narayanan, G. B. E. Stewart-Jones, T. Colpitts, H. Bennett, S. Boyoglu-Barnum, W. Shi, J. I. Moliva, N. J. Sullivan, B. S. Graham, A. Carfi, K. S. Corbett, R. A. Seder, D. K. Edwards, Serum neutralizing activity elicited by mRNA-1273 vaccine. *N. Engl. J. Med.* **384**, 1468–1470 (2021). [doi:10.1056/NEJMc2102179](https://doi.org/10.1056/NEJMc2102179) Medline
86. Y. Liu, J. Liu, H. Xia, X. Zhang, C. R. Fontes-Garfias, K. A. Swanson, H. Cai, R. Sarkar, W. Chen, M. Cutler, D. Cooper, S. C. Weaver, A. Muik, U. Sahin, K. U. Jansen, X. Xie, P. R. Dormitzer, P.-Y. Shi, Neutralizing activity of BNT162b2-elicited serum. *N. Engl. J. Med.* **384**, 1466–1468 (2021). [doi:10.1056/NEJMc2102017](https://doi.org/10.1056/NEJMc2102017) Medline
87. K. R. W. Emary, T. Golubchik, P. K. Aley, C. V. Ariani, B. Angus, S. Bibi, B. Blane, D. Bonsall, P. Cicconi, S. Charlton, E. A. Clutterbuck, A. M. Collins, T. Cox, T. C. Darton, C. Dold, A. D. Douglas, C. J. A. Duncan, K. J. Ewer, A. L. Flaxman, S. N. Faust, D. M. Ferreira, S. Feng, A. Finn, P. M. Folegatti, M. Fusko, E. Galiza, A. L. Goodman, C. M. Green, C. A. Green, M. Greenland, B. Hallis, P. T. Heath, J. Hay, H. C. Hill, D. Jenkin, S. Kerridge, R. Lazarus, V. Libri, P. J. Lillie, C. Ludden, N. G. Marchevsky, A. M. Minassian, A. C. McGregor, Y. F. Mujadidi, D. J. Phillips, E. Plested, K. M. Pollock, H. Robinson, A. Smith, R. Song, M. D. Snape, R. K. Sutherland, E. C. Thomson, M. Toshner, D. P. J. Turner, J. Vekemans, T. L. Villafana, C. J. Williams, A. V. S. Hill, T. Lambe, S. C. Gilbert, M. Voysey, M. N. Ramasamy, A. J. Pollard, COVID-19 Genomics UK Consortium, AMPHEUS Project, Oxford COVID-19 Vaccine Trial Group, Efficacy of ChAdOx1 nCoV-19 (AZD1222) vaccine against SARS-CoV-2 variant of concern 202012/01 (B.1.1.7): An exploratory analysis of a randomised controlled trial. *Lancet* **397**, 1351–1362 (2021). [doi:10.1016/S0140-6736\(21\)00628-0](https://doi.org/10.1016/S0140-6736(21)00628-0) Medline
88. T. Moyo-Gwete, M. Madzivhandila, Z. Makhado, F. Ayres, D. Mhlanga, B. Oosthuysen, B. E. Lambson, P. Kgagudi, H. Tegally, A. Iranzadeh, D. Doolabh, L. Tyers, L. R. Chinhoyi, M. Mennen, S. Skelemb, G. Marais, C. K. Wibmer, J. N. Bhiman, V. Ueckermann, T. Rossouw, M. Boswell, T. de Oliveira, C. Williamson, W. A. Burgers, N. Ntusi, L. Morris, P. L. Moore, Cross-reactive neutralizing antibody responses elicited by SARS-CoV-2 501Y.V2 (B.1.351). *N. Engl. J. Med.*
89. S. M. Kissler, C. Tedijanto, E. Goldstein, Y. H. Grad, M. Lipsitch, Projecting the transmission dynamics of SARS-CoV-2 through the postpandemic period. *Science* **368**, 860–868 (2020). [doi:10.1126/science.abb5793](https://doi.org/10.1126/science.abb5793) Medline
90. J. Lan, J. Ge, J. Yu, S. Shan, H. Zhou, S. Fan, Q. Zhang, X. Shi, Q. Wang, L. Zhang, X. Wang, Structure of the SARS-CoV-2 spike receptor-binding domain bound to the ACE2 receptor. *Nature* **581**, 215–220 (2020). [doi:10.1038/s41586-020-2180-5](https://doi.org/10.1038/s41586-020-2180-5) Medline
91. Structures used for the analysis: CC12.1 (PDB: 6XC3), CC12.3 (6XC4), COVA2-04 (7JMO), B38 (7BZ5), CB6 (7C01), CV30 (6XE1), C105 (6XCN), BD-236 (7CHB), BD-604 (7CH4), BD-629 (7CH5), C102 (7K8M), C1A-B3 (7KFW), C1A-C2 (7KFX), C1A-B12 (7KFV), C1A-F10 (7KFY), P4A1 (7CJF), P2C-1F11 (7CDI), LY-CoV481 (7KMI), LY-CoV488 (7KM8), 910-30 (7KS9), 222 (7NX6), S2H14 (7JX3), COVA2-39 (7JMP), C144 (7K90), BD23 (7BYR), 2-4 (6XEY), CV07-250 (6XQK), REGN10933 (6XDG), C121 (7K8X), C002 (7K8S), P2C-1A3 (7CDJ), S2E12 (7K4N), S2M11 (7K43), S2H13 (7JV2), CT-P59 (7CM4), LY-CoV555 (7L3N), BD-368-2 (7CHH), P2B-2F6 (7BWJ), CV07-270 (6XKP), C104 (7K8U), P17 (7CWO), C110 (7K8V), C119 (7K8W), REGN10987 (6XDG), CR3022 (6W41), COVA1-16 (7JMW), EY6A (6ZDG), S304 (7JW0), S2A4 (7JVA), DH1047 (7LD1), S309 (6WPS), C135 (7K8Z), and CV38-142 (7LM8). The paratope residues of the C104 3.8-Å structure that were truncated due to weak electron density were modeled as full side chains before performing calculations.
92. D. C. Ekiert, R. H. E. Friesen, G. Bhabha, T. Kwaks, M. Jongeneelen, W. Yu, C. Ophorst, F. Cox, H. J. W. M. Korse, B. Brandenburg, R. Vogels, J. P. J. Brakenhoff, R. Kompijer, M. H. Koldijk, L. A. H. M. Cornelissen, L. L. M. Poon, M. Peiris, W. Koudstaal, I. A. Wilson, J. Goudsmit, A highly conserved neutralizing epitope on group 2 influenza A viruses. *Science* **333**, 843–850 (2011). [doi:10.1126/science.1204839](https://doi.org/10.1126/science.1204839) Medline
93. Z. Otwinowski, W. Minor, Processing of X-ray diffraction data collected in oscillation mode. *Methods Enzymol.* **276**, 307–326 (1997). [doi:10.1016/S0076-6879\(97\)76066-X](https://doi.org/10.1016/S0076-6879(97)76066-X)
94. A. J. McCoy, R. W. Grosse-Kunstleve, P. D. Adams, M. D. Winn, L. C. Storoni, R. J. Read, Phaser crystallographic software. *J. Appl. Crystallogr.* **40**, 658–674 (2007). [doi:10.1107/S0021889807021206](https://doi.org/10.1107/S0021889807021206) Medline
95. D. Schratt, S. Li, J. Rozewicki, K. Katoh, K. Yamashita, W. Volkmut, G. Cavet, D. M. Standley, Repertoire Builder: High-throughput structural modeling of B and T cell receptors. *Mol. Syst. Des. Eng.* **4**, 761–768 (2019). [doi:10.1039/C9ME00020H](https://doi.org/10.1039/C9ME00020H)
96. P. Emsley, B. Lohkamp, W. G. Scott, K. Cowtan, Features and development of Coot. *Acta Crystallogr. D* **66**, 486–501 (2010). [doi:10.1107/S0907444910007493](https://doi.org/10.1107/S0907444910007493) Medline
97. P. D. Adams, P. V. Afonine, G. Bunkóczki, V. B. Chen, I. W. Davis, N. Echols, J. J. Headd, L.-W. Hung, G. J. Kapral, R. W. Grosse-Kunstleve, A. J. McCoy, N. W. Moriarty, R. Oeffner, R. J. Read, D. C. Richardson, J. S. Richardson, T. C. Terwilliger, P. H. Zwart, PHENIX: A comprehensive Python-based system for macromolecular structure solution. *Acta Crystallogr. D* **66**, 213–221 (2010). [doi:10.1107/S0907444909052925](https://doi.org/10.1107/S0907444909052925) Medline
98. E. Krissinel, K. Henrick, Inference of macromolecular assemblies from crystalline state. *J. Mol. Biol.* **372**, 774–797 (2007). [doi:10.1016/j.jmb.2007.05.022](https://doi.org/10.1016/j.jmb.2007.05.022) Medline
99. J. Pallesen, N. Wang, K. S. Corbett, D. Wrapp, R. N. Kirchdoerfer, H. L. Turner, C. A. Cottrell, M. M. Becker, L. Wang, W. Shi, W.-P. Kong, E. L. Andres, A. N. Kettenbach, M. R. Denison, J. D. Chappell, B. S. Graham, A. B. Ward, J. S. McLellan, Immunogenicity and structures of a rationally designed prefusion MERS-CoV spike antigen. *Proc. Natl. Acad. Sci. U.S.A.* **114**, E7348–E7357 (2017). [doi:10.1073/pnas.1707304114](https://doi.org/10.1073/pnas.1707304114) Medline
100. C.-L. Hsieh, J. A. Goldsmith, J. M. Schaub, A. M. DiVenere, H.-C. Kuo, K. Javanmardi, K. C. Le, D. Wrapp, A. G. Lee, Y. Liu, C.-W. Chou, P. O. Byrne, C. K. Hjorth, N. V. Johnson, J. Ludes-Meyers, A. W. Nguyen, J. Park, N. Wang, D. Amengor, J. J. Lavinder, G. C. Ippolito, J. A. Maynard, I. J. Finkelstein, J. S. McLellan, Structure-based design of prefusion-stabilized SARS-CoV-2 spikes. *Science* **369**, 1501–1505 (2020). [doi:10.1126/science.abc0826](https://doi.org/10.1126/science.abc0826) Medline

101. S. Bangaru, G. Ozorowski, H. L. Turner, A. Antanasićević, D. Huang, X. Wang, J. L. Torres, J. K. Diedrich, J.-H. Tian, A. D. Portnoff, N. Patel, M. J. Massare, J. R. Yates 3rd, D. Nemazee, J. C. Paulson, G. Glenn, G. Smith, A. B. Ward, Structural analysis of full-length SARS-CoV-2 spike protein from an advanced vaccine candidate. *Science* **370**, 1089–1094 (2020). [doi:10.1126/science.abe1502](https://doi.org/10.1126/science.abe1502) Medline
102. C. Suloway, J. Pulkos, D. Fellmann, A. Cheng, F. Guerra, J. Quispe, S. Stagg, C. S. Potter, B. Carragher, Automated molecular microscopy: The new Leginon system. *J. Struct. Biol.* **151**, 41–60 (2005). [doi:10.1016/j.jsb.2005.03.010](https://doi.org/10.1016/j.jsb.2005.03.010) Medline
103. G. C. Lander, S. M. Stagg, N. R. Voss, A. Cheng, D. Fellmann, J. Pulkos, C. Yoshioka, C. Irving, A. Mulder, P.-W. Lau, D. Lyumkis, C. S. Potter, B. Carragher, Appion: An integrated, database-driven pipeline to facilitate EM image processing. *J. Struct. Biol.* **166**, 95–102 (2009). [doi:10.1016/j.jsb.2009.01.002](https://doi.org/10.1016/j.jsb.2009.01.002) Medline
104. N. R. Voss, C. K. Yoshioka, M. Radermacher, C. S. Potter, B. Carragher, DoG Picker and TiltPicker: Software tools to facilitate particle selection in single particle electron microscopy. *J. Struct. Biol.* **166**, 205–213 (2009). [doi:10.1016/j.jsb.2009.01.004](https://doi.org/10.1016/j.jsb.2009.01.004) Medline
105. J. Zivanov, T. Nakane, B. O. Forsberg, D. Kimanius, W. J. H. Hagen, E. Lindahl, S. H. W. Scheres, New tools for automated high-resolution cryo-EM structure determination in RELION-3. *eLife* **7**, e42166 (2018). [doi:10.7554/elife.42166](https://doi.org/10.7554/elife.42166) Medline
106. E. F. Pettersen, T. D. Goddard, C. C. Huang, G. S. Couch, D. M. Greenblatt, E. C. Meng, T. E. Ferrin, UCSF Chimera—A visualization system for exploratory research and analysis. *J. Comput. Chem.* **25**, 1605–1612 (2004). [doi:10.1002/jcc.20084](https://doi.org/10.1002/jcc.20084) Medline
107. A. C. Walls, Y.-J. Park, M. A. Tortorici, A. Wall, A. T. McGuire, D. Veesler, Structure, function, and antigenicity of the SARS-CoV-2 spike glycoprotein. *Cell* **181**, 281–292.e6 (2020). [doi:10.1016/j.cell.2020.02.058](https://doi.org/10.1016/j.cell.2020.02.058) Medline
108. Y. Guo et al., A SARS-CoV-2 neutralizing antibody with exceptional spike binding coverage and optimized therapeutic potentials. *Research Square* **78945** [preprint]. 14 November 2020.
109. J. Ge, R. Wang, B. Ju, Q. Zhang, J. Sun, P. Chen, S. Zhang, Y. Tian, S. Shan, L. Cheng, B. Zhou, S. Song, J. Zhao, H. Wang, X. Shi, Q. Ding, L. Liu, J. Zhao, Z. Zhang, X. Wang, L. Zhang, Antibody neutralization of SARS-CoV-2 through ACE2 receptor mimicry. *Nat. Commun.* **12**, 250 (2021). [doi:10.1038/s41467-020-20501-9](https://doi.org/10.1038/s41467-020-20501-9) Medline
110. M. I. J. Raybould, A. Kovaltsuk, C. Marks, C. M. Deane, CoV-AbDab: The coronavirus antibody database. *Bioinformatics* **37**, 734–735 (2021). [doi:10.1093/bioinformatics/btaa739](https://doi.org/10.1093/bioinformatics/btaa739) Medline
- and purified the proteins for crystallization. S.M.R., H.P., and J.K. provided CV05-163 and other antibody clones and sequences. M.J.v.G. and R.W.S. and D.R.B provided plasmids for some of the antibodies reported in (11, 20), respectively. M.Y. and X.Z. performed the crystallization, X-ray data collection, determined and refined the X-ray structures. D.H., L.P. and D.N. performed the neutralization assays and M.Y. and C.C.D.L. carried out the binding assays. A.M.J., and A.B.W. provided nsEM data and performed reconstructions. M.Y., C.C.D.L., N.C.W. and I.A.W. wrote the paper and all authors reviewed and/or edited the paper. **Competing interests:** Related to this work, the German Center for Neurodegenerative Diseases (DZNE) and Charité – Universitätsmedizin Berlin previously filed a patent application that included anti-SARS-CoV-2 antibody CV05-163 first reported in (17). **Data and materials availability:** The X-ray coordinates and structure factors have been deposited to the RCSB Protein Data Bank under accession code: 7LOP. The EM maps have been deposited in the Electron Microscopy Data Bank (EMDB) under accession codes: EMD-23466 (one bound), EMD-23467 (two bound), and EMD-23468 (three bound). This work is licensed under a Creative Commons Attribution 4.0 International (CC BY 4.0) license, which permits unrestricted use, distribution, and reproduction in any medium, provided the original work is properly cited. To view a copy of this license, visit <https://creativecommons.org/licenses/by/4.0/>. This license does not apply to figures/photos/artwork or other content included in the article that is credited to a third party; obtain authorization from the rights holder before using such material.

## SUPPLEMENTARY MATERIALS

[science.sciencemag.org/cgi/content/full/science.abh1139/DC1](https://science.sciencemag.org/cgi/content/full/science.abh1139/DC1)

Materials and Methods

Figs. S1 to S12

Tables S1 to S3

References (92–110)

MDAR Reproducibility Checklist

17 February 2021; accepted 12 May 2021

Published online 20 May 2021

10.1126/science.abh1139

## ACKNOWLEDGMENTS

We thank Henry Tien for technical support with the crystallization robot, Jeanne Matteson and Yuanzi Hua for their contributions to mammalian cell culture, Wenli Yu for insect cell culture, and Robyn Stanfield for assistance in data collection. **Funding:** This work was supported by the Bill and Melinda Gates Foundation OPP1170236 and INV-004923 INV (I.A.W., A.B.W., D.R.B.), NIH R00 AI139445 (N.C.W.), NIH P01 AI110657 (I.A.W., A.B.W., R.W.S.), R01 AI132317 (D.N. and D.H.), R01 AI142945 (L.P.), the German Research Foundation (H.P.: PR 1274/3-1, and PR 1274/5-1), Helmholtz Association (H.P.: HIL-A03 and SO-097), and the German Federal Ministry of Education and Research (H.P.: Connect-Generate 01GM1908D). R.W.S. is a recipient of a Vici fellowship from the Netherlands Organisation for Scientific Research (NWO). This research used resources of the Advanced Photon Source, a U.S. Department of Energy (DOE) Office of Science User Facility, operated for the DOE Office of Science by Argonne National Laboratory under Contract No. DE-AC02-06CH11357. Extraordinary facility operations were supported in part by the DOE Office of Science through the National Virtual Biotechnology Laboratory, a consortium of DOE national laboratories focused on the response to COVID-19, with funding provided by the Coronavirus CARES Act. **Author contributions:** M.Y., D.H., C.C.D.L., N.C.W., and I.A.W. conceived and designed the study. M.Y., C.C.D.L., N.C.W. and H.L. expressed

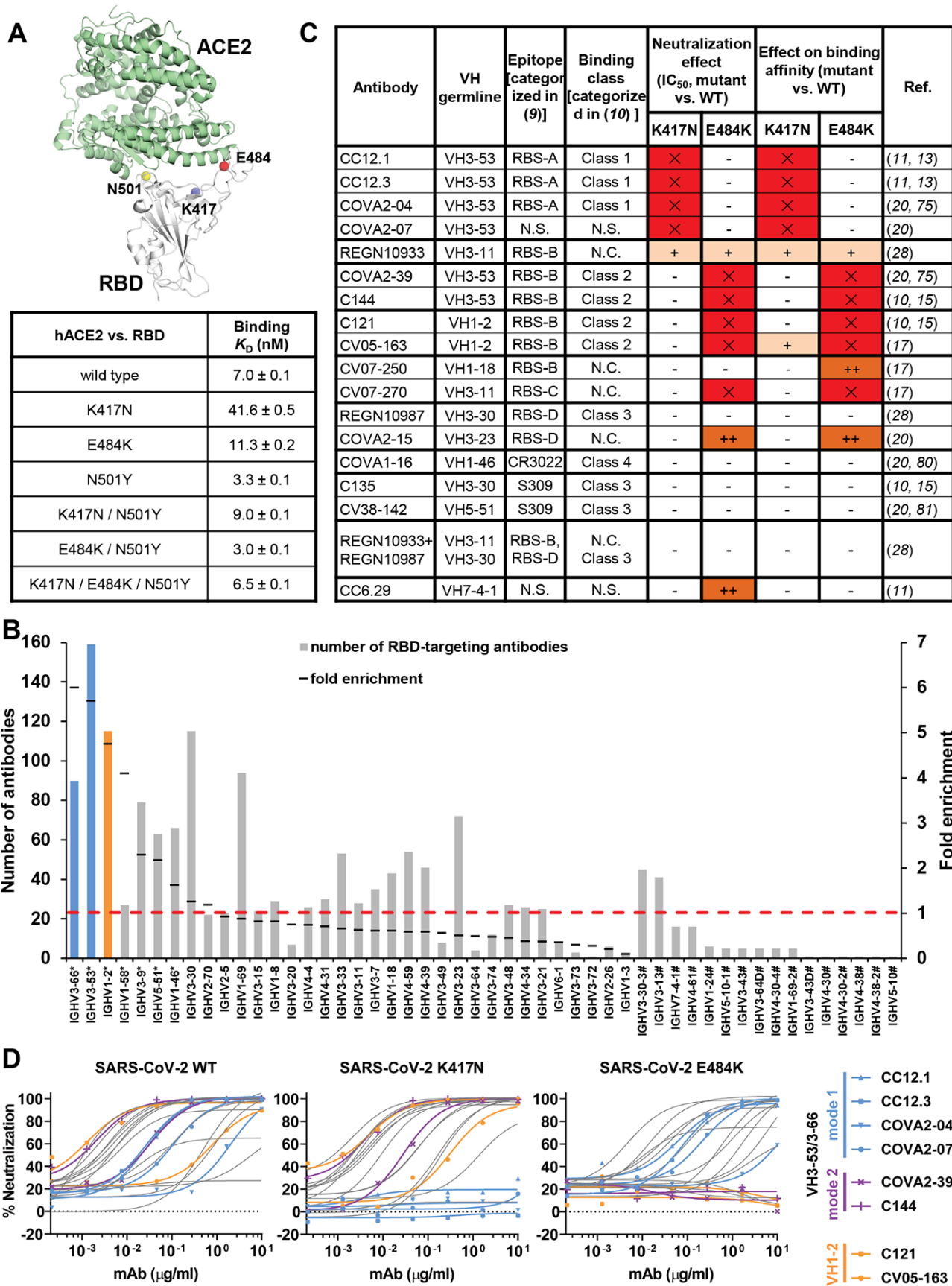


**Fig. 1 (preceding page). Emergent SARS-CoV-2 variants escape two major classes of neutralizing antibodies.** (A) Emergent mutations (spheres) in the RBS of B.1.351 and P.1 lineages are mapped onto a structure of SARS-CoV-2 RBD (white) in complex with ACE2 (green) (PDB ID: 6M0J) (90). Binding affinities of Fc-tagged human ACE2 against SARS-CoV-2 RBD wild type and mutants were assayed by biolayer interferometry (BLI) experiments. Detailed sensorgrams are shown in fig. S1. (B) Distribution of IGHV gene usage. Numbers of RBD-targeting antibodies encoded by each IGHV gene are shown as solid bars. The frequently used IGHV3-53 and IGHV3-66 genes are highlighted in blue, and IGHV1-2 in orange. The IGHV gene usage in 1,593 SARS-CoV-2 RBD-targeting antibodies (11, 14–44) compared to healthy individuals (baseline) (76) (fold-enrichment) is shown as black lines. #: IGHV gene frequencies in healthy individuals that were not reported in (76) are shown with hashtags (#). \*: IGHV genes that are significantly enriched over the baseline repertoire (76) ( $p < 0.05$ , one-sample proportion test with Bonferroni correction) are shown with an asterisk (\*). A fold-enrichment of one (red dashed line) represents no difference over baseline. (C) Effects of single mutations on the neutralization activity and binding affinity of each neutralizing antibody.  $IC_{50}$  or  $K_D$  increase that are less than 10-fold are represented by “–”, between 10- and 100-fold as “+”, and greater than 100-fold as “++”. Results in red with “X” indicate no neutralization activity or binding was detected at the highest amount of IgG used. N.C.: not categorized in the original studies. N.S.: No structure available. (D) Neutralization of pseudotyped SARS-CoV-2 virus and variants carrying K417N or E484K mutations. A panel of 17 neutralizing antibodies were tested, including four mode-1 IGHV3-53 antibodies (blue), two mode-2 IGHV3-53 antibodies (purple), and two IGHV1-2 antibodies (orange). The discrepancy between CV05-163 neutralizing SARS-CoV-2 pseudotyped virus ( $IC_{50} = 0.47 \mu\text{g/ml}$ ) and authentic virus ( $IC_{50} = 0.02 \mu\text{g/ml}$ ) reported in our previous study (17) is possibly due to different systems (pseudovirus vs. authentic virus) and host cells (HeLa cells vs. Vero E6 cells) used in these experiments.

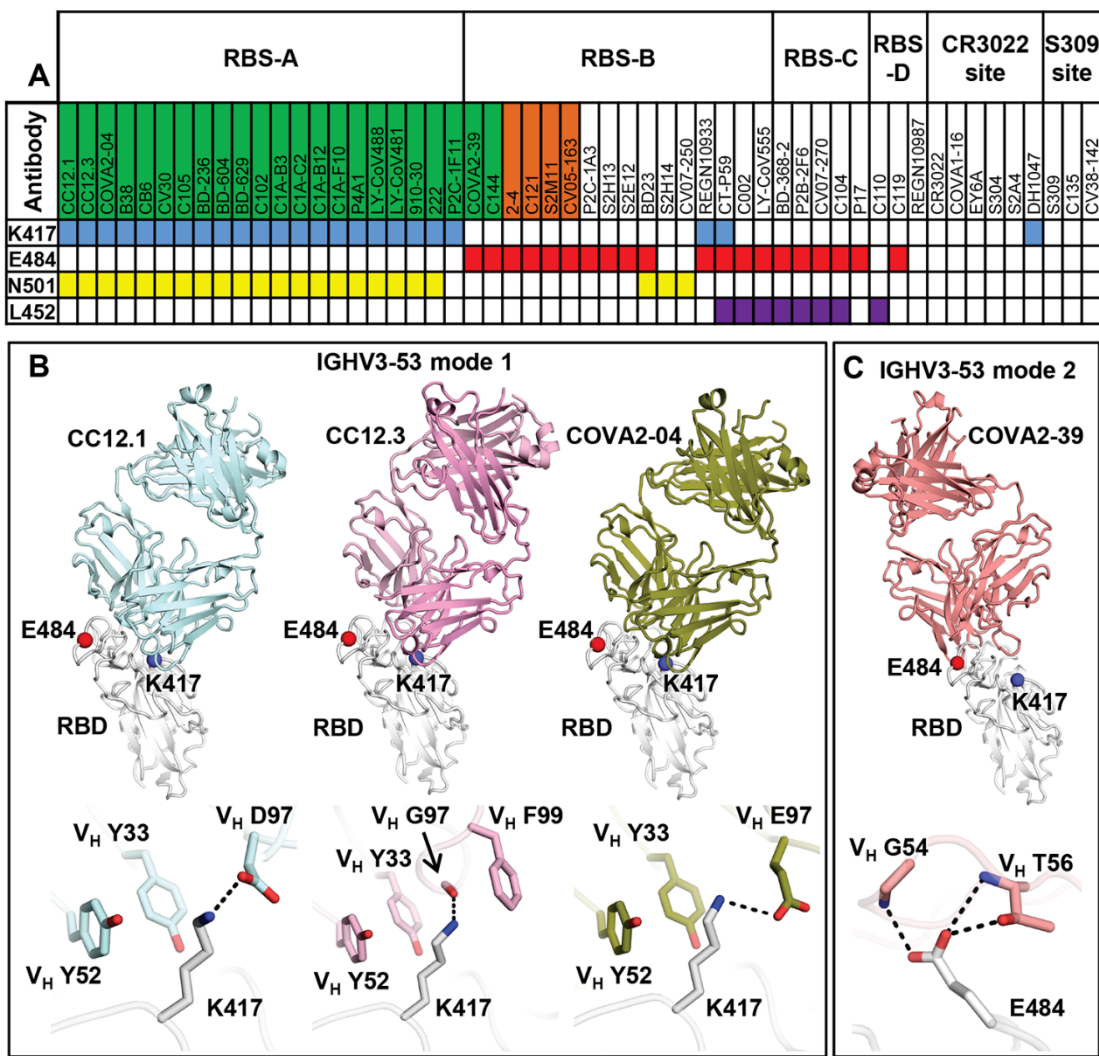


**Fig. 2. Antibody binding and structures to the wild-type SARS-CoV-2 RBS.** (A) Antibodies making contact with RBD residues K417, E484 and N501 are represented by blue, red and yellow boxes, respectively (cutoff distance = 4 Å). Antibodies encoded by the most frequently elicited IGHV3-53/3-66 and IGHV1-2 in convalescent patients are shown in green and orange boxes, respectively. Antibodies are ordered by epitopes originally classified in (9) with an additional epitope RBS-D that maps to a region in the RBS above or slightly overlapping with the S309 site. Details of the epitope classifications are shown in fig. S3A. Structures of RBD-targeting antibodies that were isolated from patients are analyzed (91). (B and C) Residues that are mutated in recently circulating variants are integral to the binding sites of IGHV3-53 antibodies. Representative structures are shown for (B) IGHV3-53 binding mode 1 [CC12.1 (PDB 6XC3), CC12.3 (PDB 6XC4) (13), and COVA2-04 (PDB 7JMO) (75)] and (C) binding mode 2 [COVA2-39 (PDB 7JMP) (75)]. The SARS-CoV-2 RBD is in white and Fabs in different colors. Residues K417 and E484 are represented by blue and red spheres, respectively. Hydrogen bonds and salt bridges are represented by black dashed lines.

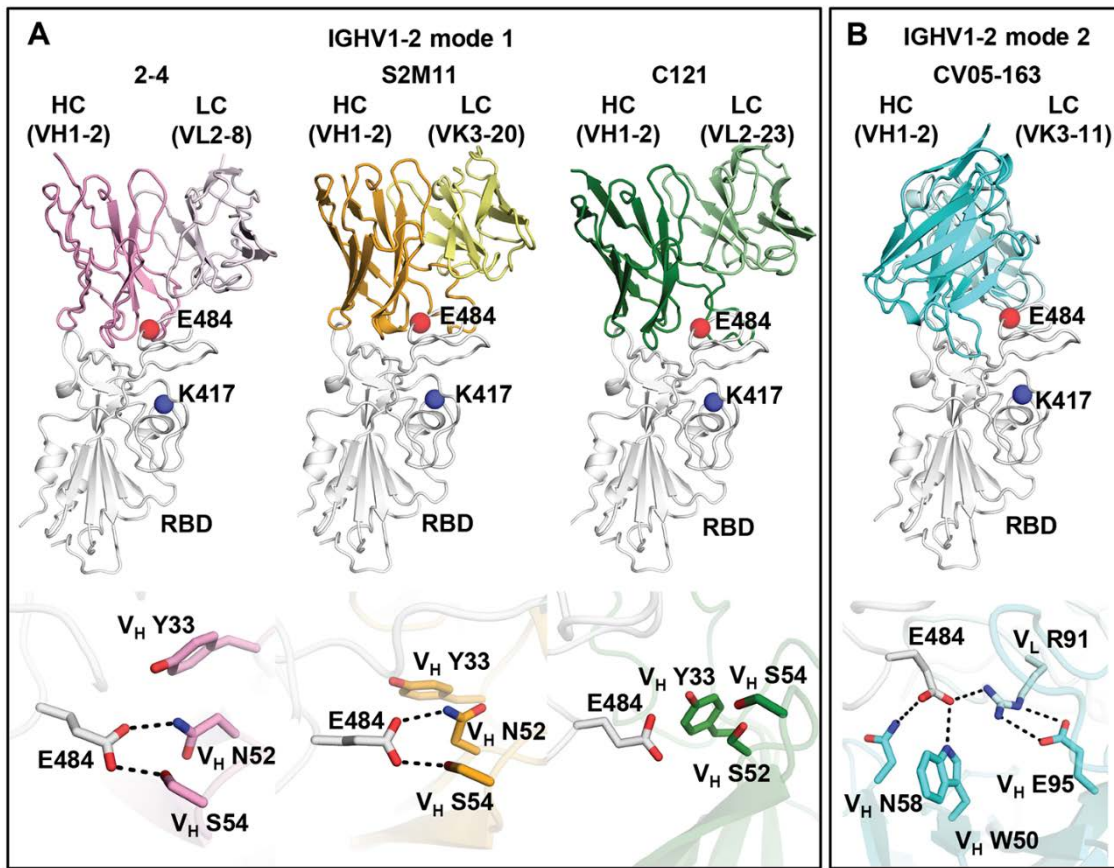


**Fig. 3. E484 is critical for RBD recognition of IGHV1-2 antibodies.** Heavy and light chains of antibody 2-4 (PDB 6XEY) (27) are shown in pink and light pink, respectively, S2M11 (PDB 7K43) (30) in orange and yellow, and C121 (PDB 7K8X) (10) in dark and light green, and CV05-163 in cyan and light cyan. The RBD is shown in white. E484 and K417 are highlighted as red and blue spheres, respectively. Hydrogen bonds are represented by dashed lines. Hydrogen bonds are not shown in the panel of C121 due to the limited resolution (3.9 Å).

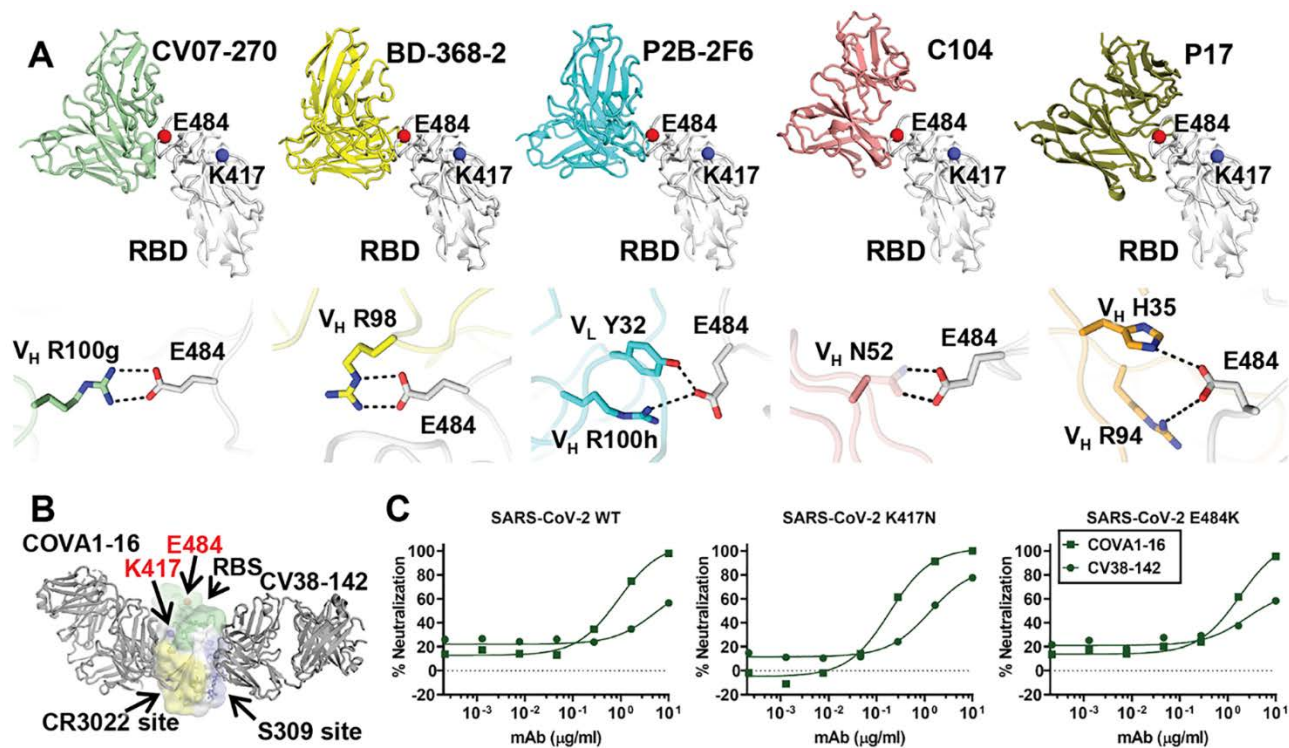


**Fig. 4. Antibodies targeting other major antigenic sites are differentially affected by mutations in recent variants.** (A) Interactions between RBS-C antibodies and SARS-CoV-2 RBD. The RBD is shown in white with E484, K417 represented as red and blue spheres, respectively. The various antibodies illustrated are in different colors. Only the variable domains are shown for clarity. Hydrogen bonds and salt bridges to E484 are represented by dashed lines. Published structures with PDB IDs 6XKP (17), 7CHF (38), 7BWJ (18), 7K8U (10), and 7CWN (78) are used to depict structures of SARS-CoV-2 RBD with CV07-270, BD-368-2, P2B-2F6, C104, and P17, respectively. The electron density for the full side chain of V<sub>H</sub> N52 was not well resolved in the 3.8-Å structure of C104 in complex with SARS-CoV-2 S. The full side chain is modeled here and shown as transparent sticks to illustrate a possible interaction with E484. (B) Cross-neutralizing antibodies to the RBD are not affected by E484 and K417 mutations. COVA1-16 targets the CR3022 cryptic site (yellow) (80) and CV38-142 targets the S309 proteoglycan site (blue) (81) to the RBD. Glycans at the N343 glycosylation site are represented by sticks. The RBS surface is shown in green. E484 and K417 are highlighted as red and blue spheres, respectively. (C) Neutralization of CV38-142 and COVA1-16 against SARS-CoV-2 wild type, K417N or E484K pseudoviruses.

## Structural and functional ramifications of antigenic drift in recent SARS-CoV-2 variants

Meng Yuan, Deli Huang, Chang-Chun D. Lee, Nicholas C. Wu, Abigail M. Jackson, Xueyong Zhu, Hejun Liu, Linghang Peng, Marit J. van Gils, Rogier W. Sanders, Dennis R. Burton, S. Momsen Reincke, Harald Prüss, Jakob Kreye, David Nemazee, Andrew B. Ward and Ian A. Wilson

published online May 20, 2021

### ARTICLE TOOLS

<http://science.science.org/content/early/2021/05/19/science.abh1139>

### SUPPLEMENTARY MATERIALS

<http://science.science.org/content/suppl/2021/05/19/science.abh1139.DC1>

### REFERENCES

This article cites 106 articles, 19 of which you can access for free

<http://science.science.org/content/early/2021/05/19/science.abh1139#BIBL>

### PERMISSIONS

<http://www.sciencemag.org/help/reprints-and-permissions>

Use of this article is subject to the [Terms of Service](#)

---

Science (print ISSN 0036-8075; online ISSN 1095-9203) is published by the American Association for the Advancement of Science, 1200 New York Avenue NW, Washington, DC 20005. The title *Science* is a registered trademark of AAAS.

Copyright © 2021 The Authors, some rights reserved; exclusive licensee American Association for the Advancement of Science. No claim to original U.S. Government Works. Distributed under a Creative Commons Attribution License 4.0 (CC BY).